Review

Journal of
Biomedical Nanotechnology
Vol. 16, 1325–1358, 2020
www.aspbs.com/jbn

Tumor Microenvironment-Specific Functional Nanomaterials for Biomedical Applications

Linlu Zhao[1], Heng Liu[1], Yanlong Xing[1], Rui Wang[1], Ziyi Cheng[1], Chuanzhu Lv[1,*], Zhiyue Lv[1,2,3,*], and Fabiao Yu[1,*]

[1] *Key Laboratory of Emergency and Trauma, Ministry of Education, Key Laboratory of Hainan Trauma and Disaster Rescue, The First Affiliated Hospital of Hainan Medical University, Institute of Functional Materials and Molecular Imaging, College of Emergency and Trauma, Hainan Medical University, Haikou 571199, China*
[2] *Key Laboratory of Tropical Translational Medicine of Ministry of Education, Hainan Medical University, Haikou 571199, China*
[3] *Key Laboratory of Tropical Disease Control (Sun Yat-Sen University), Ministry of Education, Guangzhou 510080, China*

In recent years, considerable achievements have been made to motivate the construction of tumor microenvironment (TME)-specific functional nanomaterials, which can effectively respond to the inherent pathological and physicochemical conditions in diseased regions to improve the specificity of imaging and drug delivery. Until now, various nanoarchitectures have been designed to combat cancer effectively and specifically. This review summarizes the latest developments in TME-specific theranostic nanoplatforms based on multifunctional nanomaterials that hold potential for achieving the targeted recognition at tumor sites. Recent progress and achievements have also been summarized for nanosystems that can specifically respond to the TME with various stimulus-responsive strategies and their applications for drug delivery, diagnosis, treatment, and synergistic theranostics of cancer. This review emphasizes the significance of functional nanomaterials in response to tumor stimuli to enhance anticancer treatment efficiency and facilitate development in extensive research fields, including nanoscience, biomedicine, and clinical applications.

KEYWORDS: *Functional Nanomaterials, Cancer Therapy, Tumor Microenvironment, Drug Delivery, Activable Imaging.*

CONTENTS

*Authors to whom correspondence should be addressed.
Emails: lyuchuanzhu@hainmc.edu.cn, lvzhiyue@mail.sysu.edu.cn, yufabiao@hainmc.edu.cn
Received: 4 June 2020
Accepted: 8 November 2020

INTRODUCTION

Cancer is regarded as a general term for malignant tumors, and its treatment has been a major challenge for medical research fields due to its high morbidity and mortality [1]. Generally, it is believed that cancer is caused by

the body's various carcinogenic factors, such as physical, chemical, and biological factors. Once the regulation of the normal life cycle in cells is lost, it results in uncontrolled cell proliferation and differentiation, and the cells pile up to form a tumor [2, 3]. A tumor is not an "isolated island" but an organism composed of tumor cells, multiple stromal cells, and an extracellular matrix [4]. These surrounding cells and non-cellular components form the tumor microenvironment (TME), where they interact with tumor cells and jointly promote tumor growth and metastasis [5–7]. Traditionally, the commonly used clinical treatment methods for cancer mainly include chemotherapy, radiotherapy, and surgery. However, in most circumstances, cancer cells cannot be removed completely with surgery, and both radiotherapy and chemotherapy may cause serious damage to normal human cells [8]. Compared with tumor cells, microenvironmental cells possess a stable composition, fixed specialization direction, and are

Linlu Zhao received her Ph.D. under the supervision of Professor Junqiu Liu in the State Key Laboratory of Supramolecular Structure and Materials, College of Chemistry, Jilin University in 2018. Currently she is an associate professor at the Institute of Functional Materials and Molecular Imaging, Hainan Medical University. Her main research interests include the study of detection and sensing of small molecule fluorescent probes, and development of self-assembled nanomaterials.

Heng Liu received his Ph.D. degree from University of Chinese Academy of Sciences in 2014. Then, he started to work at Hubei University. During 2017–2018, he joined Professor Ming Xian's group as a visiting scholar at Washington State University. In 2019, he moved to Hainan Medical University as an associate professor. His research interests included development of fluorescent probes and advanced molecular imaging agents.

Yanlong Xing received her Ph.D. degree from the Technical University of Berlin (TU Berlin), Germany in 2017. After her postdoctoral research in the Leibniz Institute of Analytical Science (ISAS Berlin), she joined the Hainan Medical University as a professor in August 2018. Her current research interests focus on extracellular vesicle-based liquid biopsy, microfluidic technology and the development of functional nanomaterials for biosensors.

Rui Wang received his Ph.D. degree under the supervision of Professor Jaebum Choo from Department of Bionanotechnology, Hanyang University, Korea in Feb. 2018. Then he joined Hainan Medical University in Mar. 2018. Currently he is an associate professor at the Institute of Functional Materials and Molecular Imaging, Hainan Medical University. His research interests focus on surface-enhanced Raman scattering (SERS) imaging and functional bionanomaterials.

Ziyi Cheng received his Ph.D. degree under the supervision of Professor Jaebum Choo from Department of Bionanotechnology, Hanyang University, Korea in 2019. Currently he is an associate professor at the Institute of Functional Materials and Molecular Imaging, Hainan Medical University. His research interests focus on Surface-enhanced Raman scattering based Microfluidic devices and POCT.

Chuanzhu Lv is currently a full professor, chief physician and doctoral supervisor of Hainan Medical University. He is the chairman of the Chinese Medical Association Emergency Medicine Branch and the deputy director of the Chinese Medical Association Emergency Department. In recent years, he has published more than 70 articles, succeeded in applying 9 Chinese patents and participated in the editing of 14 national textbooks. He also received 7 provincial and municipal scientific and technological progress awards.

Zhiyue Lv professor of Zhongshan School of Medicine, Sun Yat-sen University and vice president of Hainan Medcial University. He received his Ph.D. in Parasitology from Xiangya School of Medicine, Central South University, China in 2005 and completed his postdoctoral fellowship at Zhongshan School of Medicine, Sun Yat-sen University in 2007. His studies focus primarily on pathogenesis and immunoregulatory mechanism in tropical diseases.

Fabiao Yu has been a professor at the Institute of Functional Materials and Molecular Imaging, Hainan Medical University since 2017. He received his Ph.D., joint-educated, at Dalian University of Technology, and Dalian Institute of Chemical Physics, Chinese Academy of Sciences in 2013. During 2014–2017, he worked at Yantai Institute of Coastal Zone Research, Chinese Academy of Sciences. His research interests focus on fluorescence analysis and sensing, functional materials, and theranostics.

susceptible to environmental factors, which have gradually aroused the interests of researchers [9–11]. Thus, utilization of a specific TME to develop more efficient and specific techniques has been long desired to achieve satisfactory therapeutic efficacy for cancer [12, 13].

Currently, various combination therapies targeting tumor cells and multiple microenvironment cells simultaneously are being increasingly advocated for and have become a new trend in cancer diagnosis and treatment [14–18]. The emergence of nanotechnology has considerably promoted the development of cancer therapy, especially utilizing nanomaterials as drug carriers [19] to construct tumor drug delivery systems [20, 21]. Moreover, the construction of bionanomaterials based on nano-strategies offered novel ideas for the prevention, imaging, and treatment of major diseases [22, 23]. As a result of their unique physical structures and physicochemical features, nanodrug delivery systems integrate the merits of targeting recognition, a long

blood circulation time, controlled and sustained release, and stimulus-response ability, which overcome the problems of traditional pharmaceutical preparations, including poor stability, low bioavailability, short pharmacological action time, and serious adverse reactions [24–28].

The characteristic abnormalities in the TME and its cells that are different from the physiological environment of normal cells, such as high expression of enzymes, hyperthermia, acidic pH, low oxygen, and altered redox potential, have supported the idea of utilizing stimulus-responsive nanotechnologies for anticancer applications [29–32]. However, the inherently passive targeting effect and active targeting ability can considerably alleviate toxic side effects, promote selective distribution of nanomaterials in tumor tissues, and further increase efficacy [33]. Various forms, such as dendritic, spherical, caged, tubular, and rod shapes, have been established to serve as nanocarriers for drug delivery [34–36]. Additionally, the bio-nanomaterials that construct these nanostructures mainly include dendrimers, micelles, liposomes, organic and/or inorganic nanoparticles (NPs), and cell membrane-based NPs [37, 38]. According to the abundant building blocks of nanoarchitectures and the specific TME, designing smart nanomaterials with controllable structures and functions in the TME as stimuli factors will significantly improve the therapeutic effects on malignant tumors [39].

In addition to pursuing high-efficiency treatment effects, modern medicine for tumors is developing in the direction of precise visualization [40]. Based on targeted drug delivery with high specificity, accurate identification of tumor cells is also the key to achieve satisfactory efficacy. Traditional tumor-imaging techniques, including magnetic resonance imaging, ultrasound, computed tomography, X-ray, and radionuclide examination, have been widely applied in clinical practice [41–43]. Regardless, these methods still have limitations for accurately identifying early-onset and micrometastatic tumors. The emergence of molecular imaging technology has considerably promoted the development of tumor treatment [44–46]. Using optical molecular imaging navigation, even small tumors with a diameter of approximately 1 mm can be found during surgery. Thus, molecular imaging techniques provide new opportunities for the development of accurate tumor diagnosis and therapy. In particular, fluorescence bioimaging technology, with its advantages of high sensitivity, real-time intuitiveness, fast imaging, simple operation, low cost, no radioactive hazard, and simultaneous observation of multi-molecular events, has gradually become an ideal tool for studying molecular level changes in tumor cells and imaging of live animals [17, 47, 48]. With innovations in biomedicine and nanotechnology, numerous imaging contrast agents have appeared as prominent candidates for improving the target to background ratio, especially activatable imaging nanoprobes that can be specifically lit up at the targeted site [49–51]. Thus, utilizing stimulus-responsive activatable imaging probes based on nanomaterials to achieve fast and accurate diagnosis will likely result in improvements in therapeutic efficacy for cancer [52–54].

In recent decades, rapid development of various nanotechnologies and the advances in smart functional nanomaterials for precise diagnosis and efficient therapy of cancer have been forthcoming [12, 55–57]. This review discusses the most up-to-date studies on TME-specific theranostics based on multifunctional nanomaterials. Herein, we focus on targeted recognition and delivery to tumor sites, and we introduce representative nanomaterials in the field of passive and active targeting for efficient therapy. Recent progress and achievements are also summarized for nanosystems that can specifically respond to the TME, and we present various stimulus-responsive strategies and potential applications for drug delivery, diagnosis, therapy, and synergistic theranostics of cancer. Finally, the challenges and perspectives of employing TME-specific functional nanomaterials to fight cancer are discussed.

PASSIVE TARGETING STRATEGY: EPR EFFECT

Passively targeted nanomedicine is a major strategy for targeting the TME [58]. The vascular structure of normal tissues is complete, and the intercellular spaces are uniform and closely packed. It is difficult for macromolecular substances to penetrate from the blood vessels into the tissues. Tumors with abnormal proliferation have an intricate vascular network. The structure of endothelial cells is incomplete, and the gap between blood vessels and tissues is very large [59]. Additionally, the lymphatic return of the tumor site is also hindered to a certain extent, causing the retention of macromolecular substances in the tumor tissue site. This phenomenon is the most important basic properties of nanomedicine delivery systems, which is called the enhanced permeability and retention (EPR) effect (Fig. 1(a)) [60].

Combined with the pathological idiosyncrasy of solid tumors and the EPR effect, macromolecular drugs can achieve high enrichment in solid tumors, which is defined as passive tumor targeting (Fig. 1(b)). Thus, nanomedicines designed via passive targeting (the EPR effect) can significantly improve the therapeutic effect on tumors by increasing the drug concentration at the tumor site while reducing the toxic side effects on normal tissues. Many drug carriers have been designed that are clinically based on the EPR effect of solid tumor tissues (i.e., liposome drugs "Doxil" and "Onivyde," albumin-bound paclitaxel drugs "Abraxane" and "ABI-009," and polymeric micellar nanodrugs "Genexol-PM" and "NK-105") [61]. Clinical studies have shown that nanomedicine based on the EPR effect considerably reduces the chemotherapy side effects and improves the patient's quality of life [62].

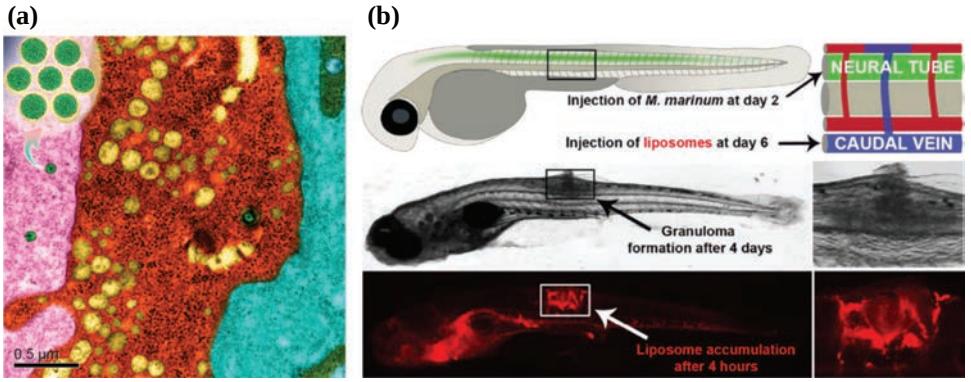

Figure 1. **(a) lipid-coated mesoporous silica nanoparticles (green pseudostained) were injected intravenously, the EPR effect of tumor tissues was manifested by a typical electron microscopy. Reprinted with permission from [63], Nel, A., et al., 2017. New insights into "permeability" as in the enhanced permeability and retention effect of cancer nanotherapeutics. *ACS Nano*, *11*(10), pp.9567–9569. Copyright@American Chemical Society. (b) Special designed NPs were applied to targeting granulomas in zebrafish embryos. The NPs using an alternative resembles the EPR mechanism to avoiding macrophage uptake. Reprinted with permission from [64], Fenaroli, F., et al., 2018. Enhanced permeability and retention-like extravasation of nanoparticles from the vasculature into tuberculosis granulomas in zebrafish and mouse models. *ACS Nano*, *12*(8), pp.8646–8661. Copyright@American Chemical Society.**

Size Effect

Overall, the geometrical size of nanomedicine affects its extravasation and accumulation in the TME [65]. The size of the nanomedicine should be larger than 5 nm to prevent it from being cleared by the kidneys and affecting the circulation time. However, NPs with a diameter of less than 20 nm are able to penetrate tumors more effectively. Thus, if nanomedicine is larger than 2000 nm, it will find it difficult to penetrate tumor blood vessels [66, 67].

Mario et al. demonstrated that ultrasmall NPs with a size less than 5 nm also displayed a good biocompatibility and biosafety profile after a 7-week period *in vivo* [68]. Similar findings have also been reported by Peng et al. They found that the performance of 5-nm NPs in tumor intratumoral transport, accumulation, and therapeutics can be increased. Their results showed that the renal clearable nanomedicine with ultrahigh vascular permeability is able to further improve the delivery of anticancer drugs without extending the blood retention time [69].

For instance, Meng et al. used a KB-31 tumor model to confirm that 50-nm mesoporous silicon NPs are better than 100 nm to achieve easier tumor enrichment via the EPR effect [70]. Sindhwani et al. examined the circumstances of NP tumor permeability by analyzing different mouse and human tumor models. AuNPs of three sizes (15, 50, and 100 nm) were used, and they found that transendothelial pathways were the dominant mechanism for NP transportation into the TME [71].

Surface Properties of NPs

Surface modification has been widely used to extend blood circulation time and increase the EPR effects of nanomedicine. The surface charge of nanocarriers affects the adsorption of proteins in plasma, thereby leading to their recognition, phagocytosis, and clearance by macrophages, which in turn affects their biological distribution in the body. Due to the negatively charged surface of blood vessels, positively charged NPs will be directly removed because they are easily adsorbed on the inner walls of blood vessels [72]. Negatively charged particles are more likely to be enriched in the liver due to selective charge filtration [73]. To prevent the NPs from being removed by a biological system, a common strategy is to modify the polymer layer or cell membrane that resists surface protein adsorption [74]. Polyethylene glycol (PEG) is an Food and Drug Administration (FDA)-approved nanomedicine that enhances surface hydrophilicity and reduces protein adsorption [75].

Chen et al. showed that the in presence of anti-PEG antibodies of patients, sometimes serious side effects can occur. The anti-PEG IgG in patients also induced an expeditious release of drugs encapsulated in nanomedicine [76]. To improve the biocompatibility of PEGylated nanomedicine, Jain et al. explored a bovine milk-derived protein (succinylated β-lactoglobuline) as an alternative strategy. It was found that the nanomedicine was stable for 30 days along with improved blood compatibility, low macrophage uptake levels, and reduced *in vitro* cytotoxicity [77].

Another strategy is to employ the membranes of platelets, white blood cells, red blood cells, cancer cells, and other cells to encapsulate the drug and design biomimetic nanomedicine carriers to avoid phagocytosis from macrophages [78]. A cell membrane-camouflaged nanomedicine was fabricated and provided new insight for efficient in situ breast cancer treatment. The stem cell membrane vesicle was engineered by paclitaxel and poly(lactide-co-glycolide). This system showed excellent stability *in vitro*, more controlled PTX release, and more effective antitumor effects [79].

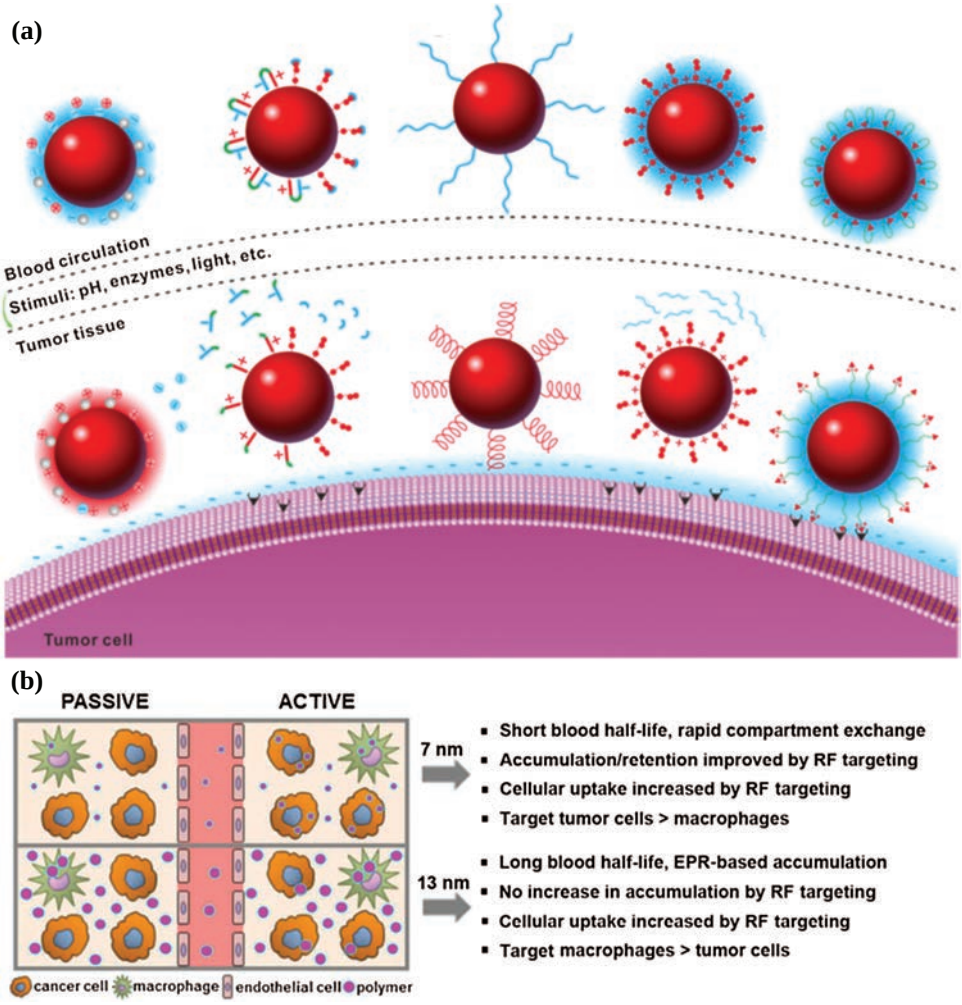

Figure 2. **(a) Active targeting nanosystems with stimuli-responsive for specific tumor targeting. Reprinted with permission from [83], Wang, S., et al., 2016. Stimuli-responsive programmed specific targeting in nanomedicine. *ACS Nano*, *10*(3), pp.2991–2994. Copyright@American Chemical Society. (b) Nanomedicine with appropriate sizes revealed balanced capability in regard to tissue penetration, EPR-based accumulation and active tumor targeting performance. Reprinted with permission from [84], Tsvetkova, Y., et al., 2017. Balancing passive and active targeting to different tumor compartments using riboflavin-functionalized polymeric nanocarriers. *Nano Letters*, *17*(8), pp.4665–4674. Copyright@American Chemical Society.**

ACTIVE TARGETING ULTILIZING TME-SPECIFIC MOLECULAR MARKERS

The delivery of nanomedicine is implemented via a "passive targeting" EPR effect or via "active targeting" owing to various ligands which conjugated to the surface of NPs. The systemic delivery of nanomedicine in multiple biological steps can affect the EPR effect and its therapeutic function, such as nanomedicine-protein interactions, blood circulation, penetration into the perivascular TME, a high interstitial pressure, and internalization of tumor cells. Compared with passive targeting nanosystems, active targeting can significantly increase the capacities of drugs delivered to target tumors [61]. Nanomedicine designed based on the EPR effect can achieve passive enrichment of the tumor site but still faces the dilemma of penetrating the tumor tissue, which can severely limit the killing effect of the drug, resulting in unsatisfactory tumor treatment effects. To overcome this issue, with improved research on the TME, studies have found that tumor tissues specifically and highly express certain proteins or receptors that are different from normal tissue levels [80]. Using the advantage of the distinct physiological environment between tumor tissue and normal tissue, the TME-specific, and highly expressed protein or ligand corresponding to the receptor is modified on the nanomedicine, thereby enhancing the interaction between the drug carrier and the cell (Fig. 2(a)). This is called active targeting by utilization of TME-specific biomarkers [81]. Targeting tumor tissues (including tumor cells and TME) by adding specific binding ligands has become a prevalent strategy to subdue the limitations of EPR-based nanomedicine (Fig. 2(b)) [82].

Targeting Tumor Blood Vessels

Tumor angiogenesis is an important feature in tumor growth and metastasis. The vascular endothelial growth factor (VEGF) receptor is an important signal protein that can induce angiogenesis in solid tumors [85]. Anti-VEGF monoclonal antibodies and other VEGF blockers have been developed, which successfully slow the growth of tumors by inhibiting tumor angiogenesis. Goel et al. proposed using mesoporous silica nanoparticles (MSNs) to target VEGF receptors. Through a comparison, they found that the targeted MSNs were three times more enriched in human glioblastoma (U87MG) than non-targeted NPs. They were further modified with the macrocyclic chelating agent, NOTA, and labeled with ^{64}Cu to achieve PET imaging [86].

$\alpha_v\beta_3$ integrin is another important tumor vascular endothelial cell receptor. It is generally expressed on the surface of vascular endothelial cells in fast-growing tumors [87]. $\alpha_v\beta_3$ integrin plays an important role in mediating the interaction between tumor cells or between cells and the matrix [88]. Several studies have emphasized the integration of integrin-targeted nanomedicine for cancer diagnosis and treatment. For instance, Zhu et al. presented active RGD-targeting metal@SiO_2 NPs, which could specifically bind to the overexpressed $\alpha_v\beta_3$ on the U87 tumor cell membrane. The constructed NPs showed noticeable thermotherapy capability in the second near-infrared (NIR-II) window, which induced photothermal-triggered cancer cell death [89].

Target Cancer-Associated Stromal Cells

Cancer-associated fibroblasts (CAFs) and tumor-associated macrophages (TAMs) are the most plentiful stromal cells in tumor tissues and are frequently used as targets for cancer treatment [90]. Various extracellular matrix (ECM) components are produced by CAFs in bulk near tumor tissues. However, TAMs are believed to affect the tumor matrix by producing proteolytic enzymes and matrix-associated proteins. TAMs are also a key builder of the tumor collagen matrix by regulating CAFs [91].

The desmoplastic stroma is known for its major barrier in the delivery of therapeutic NPs. Researchers have employed NPs in fibroblasts via in situ modification, and these NPs could be exploited as a CAFs-related apoptosis-inducing ligand in desmoplastic cancers [92]. Ernsting et al. showed that docetaxel-conjugated carboxymethylcellulose NPs were capable of depleting CAFs, thereby improving the efficacy in patient-derived post-surgical metastasis [93]. NPs reaching the tumor site are mainly blocked by CAFs and TAMs. The dense network of ECM considerably hinders their penetration in the tumor mass. Tan *et al.* designed a bio-inspired lipoprotein NP to load a photothermal agent and anticancer drug with enhanced cancer cell accessibility [91].

Targeting Tumor Metastasis Organs

The dissemination of tumor cells occurs via two mechanisms: single-cell spread through the epithelial–mesenchymal transition or collective spread of tumor clusters [94]. Targeting NPs to the metastasis site can be classified into two paces. The main target is guiding the NPs to specific organs where metastasis occurs. Secondary targeting involves targeting NPs to tumor cells or specific subcellular locations within tumor cells [95].

Tumor metastasis often occurs in the liver, lymph nodes, and lungs owing to their abundant blood vessels. Recent studies have found that the delivery of siRNA into hepatocytes must first pass through the pores of the liver endothelium [96]. Rychahou et al. demonstrated the therapeutic potential of multifunctional RNA NPs in targeting metastatic cancer cells, and their results showed the latency of these NPs as a drug delivery system for the treatment of colorectal cancer-related metastasis [97].

DESIGN OF ACIDIC TME-RESPONSIVE NANOTHERANOSTICS

Over recent decades, mounting research has demonstrated that the TME exhibits significantly different characteristics, especially an acidic pH. Compared to normal cells and tissues, tumors contain oxygenated and hypoxic regions that translate ATP to a large amount of lactic acid, which promotes the acidification of the extracellular TME in the pH range of 6.5–6.8 [98]. This unique pathway of energy production helps the tumor cells adapt to the low oxygen environment and acidic surrounding microenvironment, further promoting tumor invasion. Due to the general existence of acidic pH in most solid tumors, the acidic TME was selected as promising for tumor imaging and therapy; it has high sensitivity and selectivity, leading to rapid development of tumor diagnosis and therapy [30]. In recent decades, with the rapid development of nanomaterials and nanotechnology, many efforts have been devoted toward designing various pH-sensitive nanomaterials, which are stable at a physiologically pH of 7.4 but degrade to release the active drug in target tumor cells and tissues [99]. In this section, we will introduce the recent progress in the design of new multifunctional nanotheranostics for imaging and efficient therapy.

Imaging

Optical imaging has attracted considerable attention from researchers owing to non-invasive and real-time feedback, which generates an image through the detection of photons from fluorescent or luminescent probes in target regions [100, 101]. Among the optical imaging nanoprobes, fluorescent imaging nanoprobes have been widely applied in biological and biomedical fields. After the reaction with various targets or stimuli, the fluorescence signal can be observed directly by the detection system at a high resolution [102].

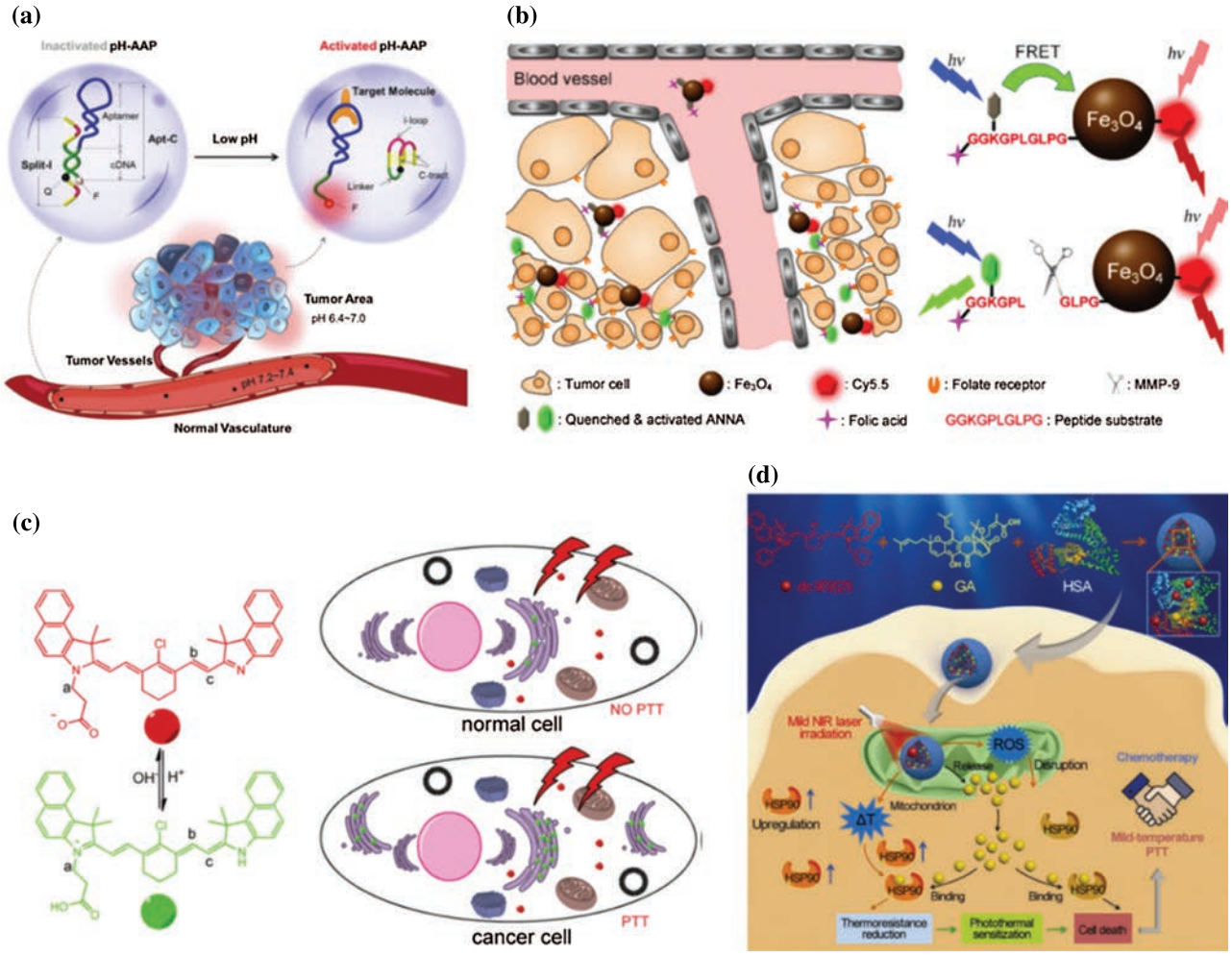

Figure 3. **(a) Scheme of pH-responsive split i-motif for tumor imaging. Reprinted with permission from [104], Lei, Y., et al., 2018. Ultra-pH-responsive split i-motif based aptamer anchoring strategy for specific activatable imaging of acidic tumor microenvironment. *Chemical Communications*, *54*(73), pp.10288–10291. Copyright@The Royal Society of Chemistry. (b) The protease and pH target-triggered fluorescent probe for tumor microenvironment imaging. Reprinted with permission from [146], Gao, M., et al., 2018. *J. Am. Chem. Soc., 140*, p.1. Copyright@American Chemical Society. (c) Illustration of pH-PTT for Golgi activated cancer therapy. Reprinted with permission from [109], Xue, F., et al., 2017. A smart drug: A pH-responsive photothermal ablation agent for Golgi apparatus activated cancer therapy. *Chemical Communications*, *53*(48), pp.6424–6427. Copyright@The Royal Society of Chemistry. (d) Scheme of HSA/dc-IR825/GA NPs for synergistic mild-temperature PTT and chemotherapy. Reprinted with permission from [111], Gao, G., et al., 2019. Molecular targeting-mediated mild-temperature photothermal therapy with a smart albumin-based nanodrug. *Small*, *15*(33), pp.1–15. Copyright@Wiley.**

To design successful fluorescent imaging nanoprobes, the "off–on" type is optimized to improve the optical performance, which implies that the signal in the responsive probe is quenched and can be activated to the fluorescent state [103]. Owing to the unique characteristics of the acidic pH in most solid tumors, designing pH-responsive fluorescent nanoprobes is promising for monitoring tumors and the TME. More pH-responsive nanoprobes have been reported based on various pH-responsive mechanisms.

Recently, Wang and coworkers developed a promising strategy for imaging acidic TME based on aptamer anchoring. The pH-activatable aptamer probe was constructed using two DNA strands (Fig. 3(a)), Split I and Apt-C [104]. Split I was labeled by a quencher, and Apt-C was conjugated with a fluorophore. In a normal pH environment, the aptamer probe is stable, leaving the quenched fluorescence of fluorophore due to its proximity to the quencher. However, the fluorescence could be recovered because of the remaining protonated overhangs from Apt-C. Subsequently, pH-activatable, cytomembrane-anchored cancer imaging could be achieved in the pH response range of 6.4–7.0. Then, this group further developed a similar pH-activatable aptamer probe for pH imaging in living cells via a combination with an acid-labile acetal linker as the responsive group [105].

The tumor-related proteases and acidic TME play important roles in cancer invasion and progression, which can be used as specific indicators for diagnosis and

therapy [106]. A dual-target responsive fluorescent probe was fabricated to visualize the distribution of matrix metalloprotease-9 activity and the pH in tumors simultaneously, which comprised pH fluorescent dye ANNA, an internal reference dye Cy 5.5, a specific linker for the connection of a peptide substrate, tumor recognition unit folic acid, and Fe_3O_4 NPs (Fig. 3(b)) [146]. Here, ANNA was conjugated with the Fe_3O_4 NPs through the metalloprotease-9 peptide substrate, and its fluorescence was quenched. Upon reaction with metalloprotease 9, the peptide linker was cleaved, indicating the ON-state for the fluorescence of ANNA, which could be used for sensing the pH of tumors. Due to the constant ON-state, Cy 5.5 served as an internal reference together with ANNA for quantitative visualization of metalloprotease 9 activity using a mouse model of human colon cancer.

Photothermal Therapy

Photothermal therapy (PTT) harvests and transforms light energy into the hyperthermia using photothermal transduction agents (PTAs) to eliminate cancer cells efficiently [107, 108]. Compared to conventional therapy, PTT has unique advantages, including noninvasiveness and controlled damage to cancer cells. PTAs can accumulate in the tumor via an EPR effect and activate targeting to enhance PTT outcomes. Currently, various kinds of PTAs have been developed to improve the photothermal conversion efficiency.

Yi et al. reported a pH-responsive PTA (BSA-pH-PTT) based on the self-assembly between asymmetric cyanine dyes and bovine serum albumin (BSA) for PTT, which can sensitively monitor pH in the range of 6.2–7.5 (Fig. 3(c)) [109]. BSA-pH-PTT could accumulate in the Golgi apparatus in cancer cells due to the hypertrophic morphology of the Golgi complex, indicating that BSA-pH-PTT could serve as a powerful tool to eliminate the cancer cells under NIR irradiation.

To improve the performance of photothermal agents, a pH-responsive photothermal nanoconjugate graphene oxide (GO)-cypate was reported for the first time to enhance PTT efficiency in the lysosomal environment [110]. In that study, GO, which has an excellent photothermal conversion efficiency, and the cyanine dye was selected to fabricate a fluorescence resonance energy transfer (FRET) system, and they served as the model receptor and donor, respectively. The cypate-grafted GO exhibited a pH-dependent FRET effect and pH-responsive photothermal in the lysosomes, which induced severe cell damage owing to the enhanced PTT.

PTT usually requires a relatively high temperature (>50 °C) for efficient cancer cell damage, which inevitably causes unnecessary effects on normal tissues. In addition, various factors affect PTT efficiency including tumor retention and liver accumulation, which decrease the amount that reaches tumor cells.

To overcome the limitations, a smart nanoagent (HSA/dc-IR825/GA NPs) was constructed via the self-assembly of human serum albumin, cyanine dye, and gambogic acid for targeted mild-temperature PTT, which could decrease the side effects to surrounding tissues (Fig. 3(d)) [111]. The fabricated HSA/dc-IR825/GA NPs exhibited an acidic pH-responsive property, pinpointing the tumor-specific location. Additionally, gambogic acid molecules blocked the stress overexpression of HSP90, thereby decreasing the thermoresistance of the cancer cells and further realizing efficient PTT at a mild temperature (<45 °C).

Photodynamic Therapy

Photodynamic therapy (PDT), as a powerful and efficient therapy modality for tumors, holds great promise for clinical applications [112, 113]. In the PDT process, photosensitizers can generate singlet oxygen to kill cancer cells through the irradiation by an appropriate laser. Due to the unique advantages of PDT including less damage to normal tissues, various nanoplatforms have been developed to improve PDT efficiency.

As an O_2-dependent treatment, PDT efficiency is often limited in clinical applications due to the hypoxic TME. To overcome this obstacle, pH-responsive aerobic NPs were successfully developed based on catalase as an O_2-evolving unit and chitosan as aerobic carriers for PDT (Fig. 4(a)) [114]. Then, the hydrophobic chlorin e6 (Ce6) was encapsulated into the NPs to obtain the photosensitizer catalase and chitosan-Ce6, which exhibited rapid pH responsiveness and excellent cellular uptake. Due to the weak electrostatic interaction, the disassembly of the PDT agent resulted in the accelerated release of catalase and Ce6 upon irradiation in the acidic microenvironment. This property considerably improved the performance of PDT for the treatment of cancer in a hypoxic microenvironment.

PDT efficiency is usually affected by limited tumor penetration of the photosensitizer and tumor hypoxic microenvironment. Liu et al. presented a pH-responsive smart nano-photosensitizer based on a self-assembly method, HAS-Ce6/TAM, by mixing Ce6-conjugated HSA with a hydrophobic drug, tamoxifen (TAM), and HAS-Ce6/TAM displayed prolonged blood circulation and increased tumor accumulation [115]. Once it enters the tumor cells, TAM is pronated to induce a transformation from hydrophilicity. Then, individual HAS-Ce6 complexes are released to enhance intertumoral penetration. Simultaneously, TAM reduces the oxygen consumption of the tumor cells by activating the AMPK pathway, which considerably improves the PDT efficacy.

A pH-sensitive PDT nanoagent that reduced the inevitable phototoxicity and was composed of self-assembled photosensitizer-grafted polymeric ligands and upconversion nanoparticles (UCNPs) was reported by Ling's group [116]. Under neutral pH conditions, the PDT

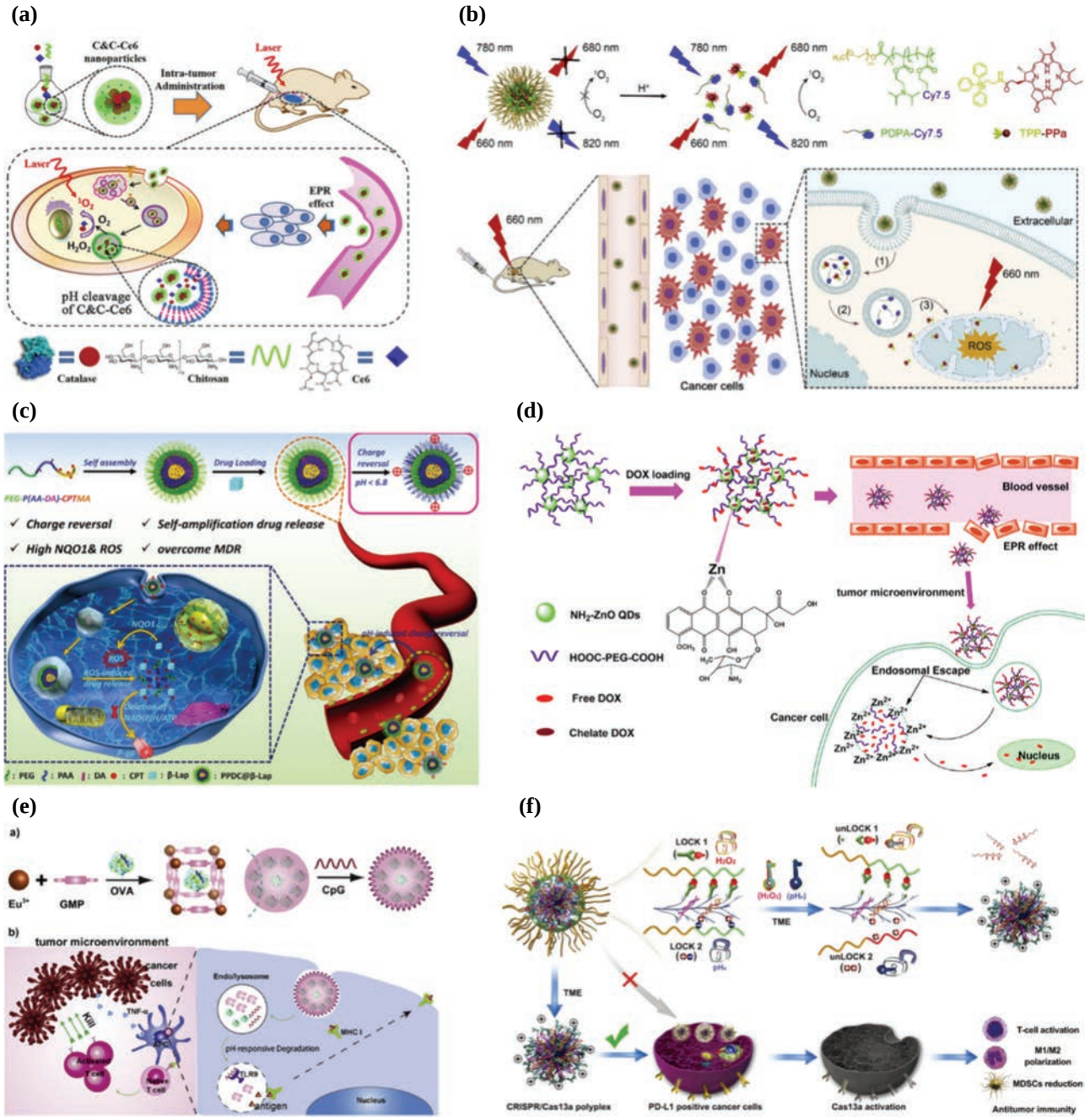

Figure 4. (a) Scheme of self-assembly for catalase and chitosan-Ce6 (C&C-Ce6) NPs for effective PDT. Reprinted with permission from [114], Shen, L., et al., 2017. pH-responsive aerobic nanoparticles for effective photodynamic therapy. *Theranostics*, *7*(18), pp.4537–4550. Copyright@Theranostics. (b) Illustration of M-TPPa for early endosome- and mitochondria-targeting of PDT. Reprinted with permission from [118], Qi, T., et al., 2019. A pH-Activatable nanoparticle for dual-stage precisely mitochondria-targeted photodynamic anticancer therapy. *Biomaterials*, *213*, pp.1–12. Copyright@Elsevier. (c) Illustration of the PPDC system for chemotherapy in vivo. Reprinted with permission from [120], Dai, L., et al., 2019. A pH/ROS cascade-responsive charge-reversal nanosystem with self-amplified drug release for synergistic oxidation-chemotherapy. *Advanced Science*, *6*(4), pp.1–13. Copyright@Wiley. (d) Scheme of preparation of the PEG-cZnO delivery system. Reprinted with permission from [122], Cai, X., et al., 2017. pH-Responsive ZnO nanocluster for lung cancer chemotherapy. *ACS Applied Materials & Interfaces*, *9*(7), pp.5739–5747. Copyright@American Chemical Society. (e) Scheme of pH-responsive metal-organic frameworks for enhanced cancer immunotherapy. Reprinted with permission from [126], Duan, F., et al., 2017. A simple and powerful co-delivery system based on pH-responsive metal-organic frameworks for enhanced cancer immunotherapy. *Biomaterials*, *122*, pp.23–33. Copyright@Elsevier. (f) Schematic representation of dual-locking nanoparticles for efficient immunotherapy. Reprinted with permission from [128], Zhang, Z., et al., 2019. Dual-locking nanoparticles disrupt the PD-1/PD-L1 pathway for efficient cancer immunotherapy. *Advanced Materials*, *31*(51), pp.1–10. Copyright@Wiley.

nanoagents were negatively charged in the self-quenched state; however, once they entered into the tumor acidic microenvironment, their surface charge switched from negative to positive. Subsequently, the PDT nanoagents were further disassembled into individual UCNPs in tumor cells (pH∼5.5). Upon near-infrared irradiation, the efficient PDT could be realized in tumor cells because of the photoactivity of the free PDT nanoagents.

Due to the short lifetime and irradiation dependence of $^1O_2$, the cytotoxic region could be confined in the irradiated regions, allowing confined therapeutic efficacy. To reduce the unfavorable photochemical damage, a new PDT agent based on an organic–inorganic hybrid nanocarrier was developed for photodynamic treatment of cancer cells, which comprised calcium/phosphate ions (CaP), Ce6, and poly(ethylene glycol)-*b*-poly(aspartic acid) [117]. CaP as the core of the hybrid nanocarrier encapsulated the PSs with a PEG layer. Under pH 7.4 conditions, the photochemical activity of the nanocarrier could be suppressed. Under acidic conditions of endo-/lysosomes, PDT could be realized.

To enhance the therapeutic outcome of mitochondria-targeted PDT, new pH-activatable NPs were developed with a targeting capacity for PDT efficacy (Fig. 4(b)) [118]. mPEG-*b*-PDPA-Cy7.5 could self-assemble into the NPs to render a sharp pH response. The fluorescent signal of Cy7.5 was suppressed due to the HOMO-FRET from pyropheophorbide-a to Cy7.5, which induced self-quenching. Under normal physiological conditions, the M-TPPa remains silent; however, after tumor accumulation and intracellular uptake, the fluorescent signals of M-TPPa could be activated due to immediate dissociation. Subsequently, TPPa could translate from the early endosome to mitochondria. Finally, the relocated TPPa generated O_2 to efficiently kill cancer cells upon laser irradiation, leading to improved treatment efficiency and reduced systemic adverse effects.

Chemotherapy

Chemotherapy as the important primary mode of cancer therapy has attracted increasing attention [119]. The severe cytotoxicity of drugs is one of the major obstacles, limiting their clinical applications. To reduce the drugs' side effects, various strategies for chemotherapy drug delivery have been developed, including protein-based NPs. Wang et al. fabricated a new platform of folate (FA)-conjugated sericin NPs for release of doxorubicin (DOX), which exhibited cancer-targeting capability. The self-assembly of sericin-DOX nanocomposites would be promoted. Then, FA was selected as a cancer-targeting unit to actively bind the overexpressed folate receptors and covalently graft them to SND nanocomposites, which aided the FA-SND NP endocytose into the lysosome.

Cellular uptake of drugs directly affects the efficiency of therapy. To improve the therapeutic effect, a new micelle drug delivery system was constructed utilizing pH/reactive oxygen species (ROS) cascade-responsive prodrug for efficient cancer therapy, which exhibited excellent performance by encapsulating β-lapachone (Fig. 4(c)) [120]. In an acidic microenvironment, the tumor cell uptake could be enhanced. Subsequently, the dissociation of the micelle system under ROS stimulation induced the release of drugs, which could produce ROS upon the catalysis of nicotinamide adenine dinucleotide (NAD) (P)H: quinone oxidoreductase-1 (NQO1). Moreover, the ROS synergized with CPT and further propagated tumor cell apoptosis, which provided a powerful antitumor tool.

Similarly, Ji et al. prepared IR-780-labeled prodrug micelles to improve the therapeutic effect and avoid drug resistance in cancer therapy [121]. In an acidic TME, the prodrug micelles exhibited fast DOX release but remained stable in physiological conditions. The combination of the hyperthermia effect under NIR laser irradiation and pH-responsive drug release significantly increased the intracellular DOX accumulation and induced cancer cell apoptosis.

In the past few years, quantum dot cluster-based drug delivery systems (DDSs), which can penetrate through leaky vessels and increase the accumulation amount in tumor tissues via the EPR effect, have attracted considerable attention. Compared to large NPs, clusters based on small NPs exhibit better biodegradability and larger surfaces for the conjugation of drugs. A pH-responsive anticancer DDS that loaded large amounts of DOX was constructed using small single ZnO QDs through cross linking of PEG (Fig. 4(d)) [122]. Upon cellular uptake by tumor cells, the metal–drug complex was disassembled, and the drug was efficiently released due to the carrier's complete dissolution and pH-sensitive response. The additional cytotoxicity of Zn^{2+} after post dissolution combined with the chemotherapy of DOX preferentially killed cancer cells.

Immunotherapy

Immunotherapy, as a new type of cancer treatment for clinical applications, has attracted increasing attention. Unlike direct therapeutic strategies, including chemotherapy, radiotherapy, and surgery, immunotherapy as an indirect method stimulates the host's own immune system to fight a specific cancer or removes immunosuppress ions, and it has attracted considerable attention as an alternative to current therapy methods [123, 124]. However, the accurate delivery of antigens into cells remains a key challenge, preventing cells from controlled modulation of the immune system due to serious adverse effects [125].

The current tumor-associated antigen delivery strategy cannot meet the requirements of clinical therapy due to low loading efficiency. Thus, a novel antigen delivery system was fabricated for cancer immunotherapy, which utilized lanthanide ions and guanine (Fig. 4(e)) [126].

Under the acidic environment, the loaded model vaccine ovalbumin could be released due to the relatively labile metal-ligand bonds, which could accelerate protein antigen escape from the endo-/lysosomes and enhance antigen cross-presentation. The pH-sensitive co-delivery system of antigens and immunostimulatory molecules could enhance the antitumor outcome in B16-ova melanoma cancers.

Imidazoquinoline-based toll-like receptor (TLR) 7/8 agonists can activate dendritic cells to secrete pro-inflammatory cytokines. Unfortunately, the small molecule agonists often suffer from rapid clearance from the injection site, which seriously decreases the *in vivo* efficacy. To overcome this obstacle, pH-responsive poly(lactide-co-glycolide) NPs have been developed to increase the novel agonist payload efficiency and improve endo-/lysosome-specific agonist release, which further resulted in stronger activation of DCs for enhanced immunotherapy [127]. Bicarbonate salt was incorporated to generate CO_2 at an acidic pH to incorporate pH responsiveness, which significantly increased the acidic pH responsiveness of the agonist.

The clustered, regularly interspaced short palindromic (CRISPR)-associated (Cas) enzyme, Cas13a, has great potential for selective elimination of cancer cells via collateral effects. Unfortunately, the specificity of the collateral effects for targeting tumor cells is not sufficient, inducing safety issues upon treatment. A dual-locking nanoparticle (DLNP) with a core-shell structure have been described to restrict CRISPR/Cas13a activation to tumor tissues through interaction with both the pHe and H_2O_2 concentrations in the TME (Fig. 4(f)) [128]. Upon entering the TME, the polymer layer could only be degraded when both acidic pHe and a high H_2O_2 concentration were present. Under careful control of gene editing in tumor cells through CRISPR/Cas13a activation, DLNP loading of CRISPR RNA (crRNA) could then accumulate in the tumors and induce the death of PD-L1-positive tumor cells.

Combined Therapy

PTT and PDT have been considered as excellent alternatives to translational tumor treatment owing to the high selectivity and lack of drug resistance, which depend on the absorbed photon energy by PTAs or PSs to generate heat or ROS, respectively, causing the death of cancer cells. The combination of PTT and PDT can considerably improve therapy efficiency for cancer. The diketopyrrolopyrrole nanoparticles (DPP-NF NPs) were developed by introducing a nitric oxide (NO) photodonor and pH-sensitive group into the DPP-NF core, which could serve as an NO delivery carrier and could be activated in the acidic TME of the lysosome to generate ROS and enhance the photothermal efficiency [129]. NO could suppress tumor growth when it was in a suitable concentration (nM to mM). Thus, under the assistance of controllable NO release, DPP-NF NPs not only triggered tumor cell death but also overcame the previous limit of PDT treatment in a tumor hypoxic microenvironment.

Malignant melanoma, as an increasing risk to skin health, has attracted increasing attention, and it exhibits resistance to conventional chemotherapy. Thus, it is urgent to develop more efficient therapeutic agents for the treatment of malignant melanoma. The new combined photothermal and photodynamic therapeutic agents have been developed with pH-responsive features using poly(N-phenylglycine) (pNPG). To improve the targeting capability of the combined agents, hyaluronic acid (HA) was introduced into the agents, which served as a specific recognition unit of CD44 that overexpresses on the surface of tumor cells [130]. As a result, HA-modified pNPG could efficiently suppress malignant melanoma tumor growth upon irradiation with a 808-nm laser, demonstrating that HA-modified pNPG could be used for the dual modality PTT/PDT of melanoma.

Current cancer chemotherapy often suffers from inefficient tumor uptake of the drug with severe side effects and inevitable multidrug resistance after a period of treatment. Combing PTT with chemotherapy provides an alternative strategy for cancer therapy owing to the satisfactory synergetic therapy of thermal treatment combined with controlled drug release.

As is well known, photothermal conversion efficiency (PCE) can be tuned through careful control of agents' morphology. A photothermal chemotherapeutic virus-like nanodrug based on acidic TME-responsive shape reversal was developed via a coordination-driven assembly to improve the NIR-II PCE (Fig. 5(a)) [131]. The virus-like nanodrug comprised a NIR-I fluorescence (IR825), an antitumor drug (PEM), and rare-earth metal (neodymium, Nd (III)) ions. Upon triggering by the acidic TME, a shape reversal could be obtained due to shell detachment, which induced the enhanced NIR-II PCE. Additionally, the disassembly of the virus-like nanodrug core could induce enhanced NIR-II photothermal chemotherapy via the precise guiding of "off–to–on" NIR-I fluorescence and "on–to–off" NIR-II photoacoustic imaging.

The combination of immunotherapy with other therapies could improve therapeutic efficiency. Thus, smart pH-responsive nanovesicles (pRNVs) were prepared via the self-assembly from the block copolymer, polyethylene glycol-*b*-cationic polypeptide (PEG-*b*-cPPT) (Fig. 5(b)) [132]. The pRNVs not only served as nanocarriers but also caused immunogenic cell death to increase the immunotherapy efficiency, which co-encapsulated the photosensitizer, 2-(1-hexyloxyethyl)-2-devinyl pyropheophorbide-a (HPPH), and the indoleamine 2,3-dioxygenase inhibitor, indoximod (IND), to fabricate the pRNVs/HPPH/ING system. Upon laser irradiation, HPPH could produce ROS to directly kill cancer cells by PDT. Moreover, host immunity could be evoked by

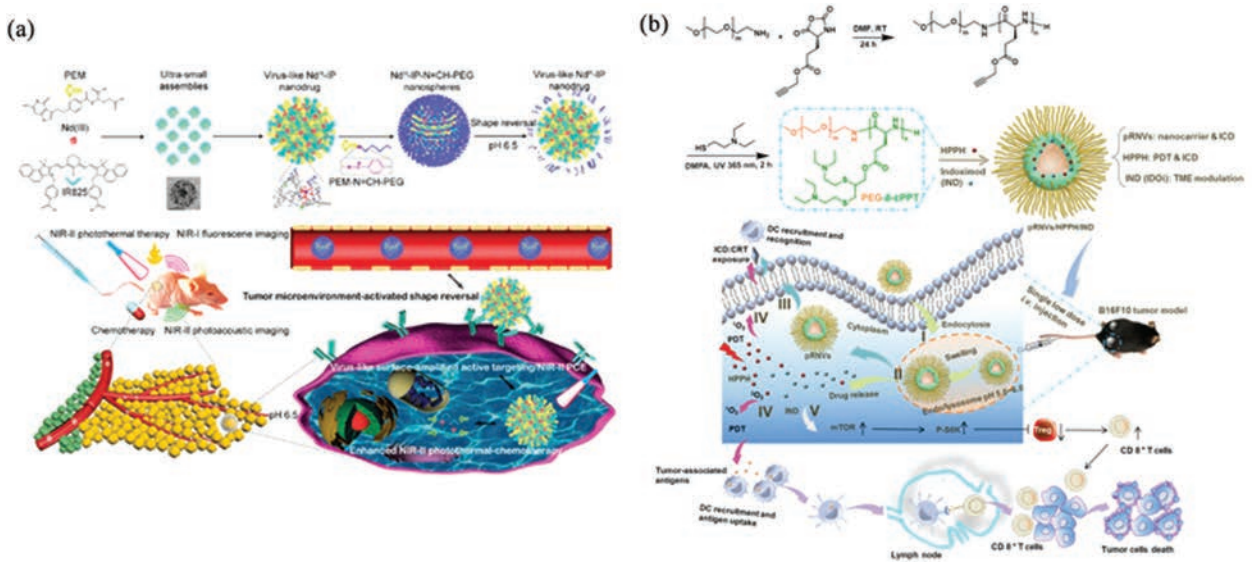

Figure 5. **(a) Illustration of the synthesis of the NdIII-IP virus-like nanodrug and its combined PTT/chemotherapy. Reprinted with permission from [131], Li, Y., et al., 2019. Tumor microenvironment responsive shape-reversal self-targeting virus-inspired nanodrug for imaging-guided near-infrared-II photothermal chemotherapy. *ACS Nano*, *13*(11), pp.12912–12928. Copyright@American Chemical Society. (b) Scheme of the construction of pH-responsive nanovesicles. Reprinted with permission from [132], Yang, W., et al., 2020. Smart nanovesicle-mediated immunogenic cell death through tumor microenvironment modulation for effective photodynamic immunotherapy. *ACS Nano*, *14*(1), pp.620–631. Copyright@American Chemical Society.**

pRNVs/HPPH/ING, which promoted DC recognition and was modulated by IND.

ENZYME-OVEREXPRESSION-INSPIRED FUNCTIONAL NANOMATERIALS

Enzymes play critical roles in most of the metabolic processes in organisms. However, the dysfunction or abnormal expression of enzymes is normally closely related to various diseases. Compared to the surrounding normal physiological tissues, the overexpression of proteases is associated with malignant tumors, resulting in a much higher concentration of enzymes in the intracellular or extracellular milieu of the tumor [133]. Thus, with the purpose of targeted bioimaging and on-demand drug release, enzyme-activatable nanosystems for real-time and in situ bioimaging, as well as anticancer drug delivery, have been attracting increasing research attention. Many DDSs have been elegantly exploited by integrating them with specific functional groups that can be selectively distinguished and degraded via the abnormal expressed enzymes in the intracellular or extracellular milieu of the tumor according to the levels of enzymes in normal tissues [134]. The most widely researched tumor-associated enzymes that can serve as promising tumor markers and enzymatic triggers for activatable nanoprobes involve matrix metalloproteinases (MMPs) [135, 136], cathepsin B [137, 138], hyaluronidase (HAase) [139], and caspase 3/7 [28, 140]. In the design of enzyme-activatable imaging nanoprobes or DDSs, enzyme-responsive moieties, e.g., peptides, have been utilized to bind the nanosubstrate with the imaging agent or drugs. Thus, the high levels of enzymes in tumor lesions can specifically control release of the imaging agent or drugs by degradation, morphology transformation, or bond cleavage [12, 141].

In this section, we focus on recent research progress on enzyme-responsive imaging nanoprobes, the enzyme-based drug delivery nanocomposites for targeted tumor therapy, and enzyme-triggered imaging-guided synergetic therapy for emerging theranostics systems [30].

Enzymatic Cleavage-Based Stimulus-Responsive Optical Nanoprobes

Fluorescence Imaging Nanoprobes

Fluorescence-based imaging nanoprobes have been widely employed for the detection of protease due to their excellent selectivity, high sensitivity, as well as multiplexed testing capability [142]. The main design principle of fluorescence imaging nanoprobes for enzyme detection are based on FRET or bioluminescence resonance energy transfer (BRET) [143]. In recent years, FRET-based bio-probes have been extensively investigated for enzyme expression detection *in vivo*. Typically, FRET-based imaging nanoprobes are composed of a fluorescence donor and a fluorescence quencher that are conjugated by an enzyme-responsive peptide linker of ∼1–10 nm. The overlapping fluorescence emission profile between the donor and the absorption of the acceptor results in energy transfer between these two moieties, resulting in donor fluorescence quenching via the acceptor, while cleavage of a certain peptide linker by a specific protease can lead to fluorescence recovery of the donor,

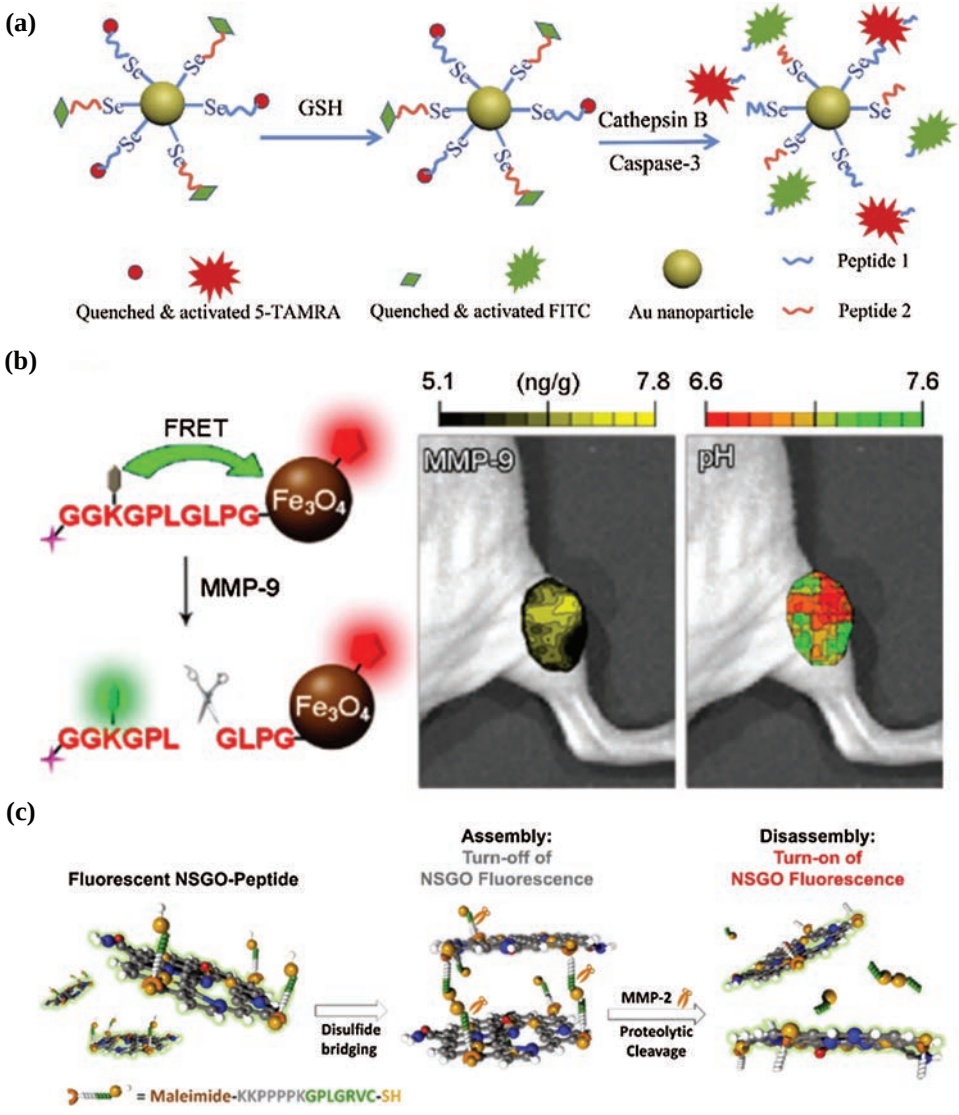

Figure 6. **(a) Illustration strategy of Au–Se nanoprobes for cathepsin B and caspase-3 in biosystems. Reprinted with permission from [143], Gao, X., et al., 2020. Real-time in situ monitoring of signal molecules' evolution in apoptotic pathway via Au–Se bond constructed nanoprobe. *Biosensors and Bioelectronics*, *147*, pp.1–8. Copyright@Elsevier. (b) The reaction mechanism and structure of the MMP-9-cleavable FRET-based nanoprobe (left) and fluorescence images of MMP-9 activity and tumor microenvironment pH. Reprinted with permission from [146], Ma, T., et al., 2018. Dual-ratiometric target-triggered fluorescent probe for simultaneous quantitative visualization of tumor microenvironment protease activity and pH in vivo. *Journal of the American Chemical Society*, *140*(1), pp.211–218. Copyright@American Chemical Society. (c) The NSGO assembly–disassembly mechanism for MMP-2 detection. Reprinted with permission from [150], Yang, J.K., et al., 2019. Atomically-tailored graphene oxide displaying enhanced fluorescence for the improved optical sensing of MMP-2, *Sensors and Actuators B: Chemical*, *284*, pp.485–493. Copyright@Elsevier.**

which can be used for the determination of the enzyme expression [142].

To date, different nanomaterials have been devised to be fluorescent donors, for instance, quantum dots and fluorescent nanomaterials. Various other nanostructures, including AuNPs [143, 144], Fe_3O_4 NPs [145, 146], two-dimensional nanomaterials [147], mesoporous silica NPs [148], and multiwalled carbon nanotubes [149], can serve as good candidates for fluorescence quenchers.

For instance, Tang et al. designed an Au–Se bond-based nanoprobe for detection of the two apoptosis biomarkers, cathepsin B and caspase 3. Two different peptides that were separately bound with two fluorescence dyes were decorated with AuNPs through Au–Se bonds. The fluorescence of the two dyes was initially quenched by AuNPs. However, when the enzymes were present, the peptide linkers could be separately cleaved via cathepsin B and caspase-3, resulting in recovered fluorescence (Fig. 6(a)). This enzyme-responsive fluorescent

nanoprobe could be used to investigate protein interactions and monitor the serial activation of intracellular signaling pathway molecules *in vivo* [143].

An MMP-9-responsive fluorescent imaging nanoprobe was reported by the Gao group based on a FRET pair of biocompatible Fe_3O_4 nanocrystals and a pH-sensitive fluorescence dye, which was bonded by a specific peptide linker. The fluorescence of the dye was quenched by the Fe_3O_4 particles, leading to the "off" state of the nanoprobe. Then, the cleavage of the peptide linker by MMP-9 for the quencher recovered the fluorescence, representing the "on" state. In that study, the fluorophore was detached together with a tumor selective antibody, which could be covalently bound within the C-terminal of the peptide linker, making pH imaging of the TME achievable [145]. Based on that study, the same group further developed a fluorescent nanoprobe for synergistic visualizing protease activity and pH. The probe exhibited a capability of dual ratiometric target-triggered and quantitative detection *in vivo*. The nanosystem was also composed of the pH-sensitive fluorophore, Fe_3O_4 NPs, ANNA, and the near-infrared cyanine Cy5.5. In addition to the above-mentioned pH imaging FRET nanoprobe, Cy5.5 was used as an internal indicator, which can form a desirable ratiometric fluorescent platform for monitoring MMP-9 activities *in vivo* (Fig. 6(b)). Further application of the developed nanoprobe to a xenograft mice model demonstrated the capability of the dual ratiometric sensor for visualizing the activity of MMP-9 as well as pH mapping *in vivo* at the same time [146]. The overexpressed protease activity and acidified extracellular pH were significant features, which had a close relation to tumor progression and invasion, as well as metastasis. Thus, developing enzyme-triggered or enzyme- and pH-activated fluorescent nanoprobes is of great importance for cancer diagnostics.

GO-based 2D nanomaterials exhibit characteristics with a larger absorption cross-section and longer-range energy transfer. Therefore, they are widely employed as fluorescence quenchers in FRET-based MMP biosensors. Separately, these kinds of 2D materials have been explored for protease detection as a result of the morphology changes of assembling/disassembling. For instance, Yim et al. fabricated heteroatom-doped GO using the atoms of sulfur and nitrogen (NSGO), which emitted higher increasing fluorescence. A NSGO assembly substrate was formed via disulfide bonds integrating the sulfhydryl-containing peptides into the NSGO, leading to fluorescence quenching for nanoassembly. However, upon coexisted with MMP-2, NSGO bundle disassembled, resulting in a high recovery of the fluorescence signals, which were used for sensitive tumor MMP-2 detection (Fig. 6(c)) [150].

SERS-Based Nanoprobes

Surface-enhanced Raman scattering (SERS) is also a crucial optical sensing technology that is widely used in the non-invasive detection of biomolecules, including proteins. SERS measures the inelastic light scattering of molecules with larger increasing signals (approximately $\geq 10^8$) when the molecules are close to Au, Ag, and other plasmonic metallic nanoparticles, as well as nanostructures [151]. SERS-based biosensors are normally composed of metallic substrates and Raman reporter molecules, which are linked by MMP-cleavable peptide linkers. For example, Gong et al. designed a SERS nanoprobe using a bimetallic film-overnanosphere substrate and AuNPs for multiplex detection of MMP activities. The substrate contained an Au–Ag bimetallic layer and was decorated with NeutrAvidin–biotin-PEG conjugates via Au–S bonds. Subsequently, AuNPs functionalized with MMP peptide substrates, biotin–PEG, and Raman reporters were supplied to the system. Upon cleaving the peptides via the specific MMP, the biotin-NeutrAvidin complexation sites were obtained. Thus, AuNPs were integrated into the substrate, resulting in increasing Raman signals [152]. In a subsequent study, Gong et al. developed an optical interference-free SERS nanoprobe for the multiplexed detection of MMPs, which was based on a similar cleave-and-bind mechanism. The nanoprobe substrates were metal (molybdenum and tungsten) carbonyl conjugate nanotags (^{Mo}CO and ^{W}CO) on a SERS-based platform. As illustrated in Figure 7, after coating the nanopillar substrates with MMP-2, MMP-7, and MMP-9-peptide-PEG, three nanotags that were ^{Mo}CO, $^{Wpph3}CO$, and $^{Wpcy3}CO$ functionalized by biotin or NeutrAvidin were bound to the SERS substrate. Here the conjugated peptide, PEG, was used to separate the nanostructures from aggregation. When the MMP enzymes were present, they could cleave the corresponding peptide linkers, resulting in a connection between NeutrAvidin and biotin of the nanotag as well as enhanced SERS signals for different MMPs [153]. In addition to SERS intensity changes, the spectral shifts in the SERS nanoprobes induced by the MMP-responsive interaction could also be applied for the detection of protease activity [154].

Magnetic Nanoprobes

Magnetic nanosensors can be used for sensitive and selective MMP detection in complex biosystems due to the negligible magnetic background of biosamples. Typically, superparamagnetic magnetic nanoparticles (MNPs) that are able to magnify the magnetic resonance of protons of water molecules and cause changes in T_1- or T_2-weighted signals act as magnetic nanoprobe substrates [155]. MNP aggregation can facilitate water proton dephasing and can result in a shift in the proton relaxation time (T_2). For example, Gandhi et al. described an outline for MMP-2

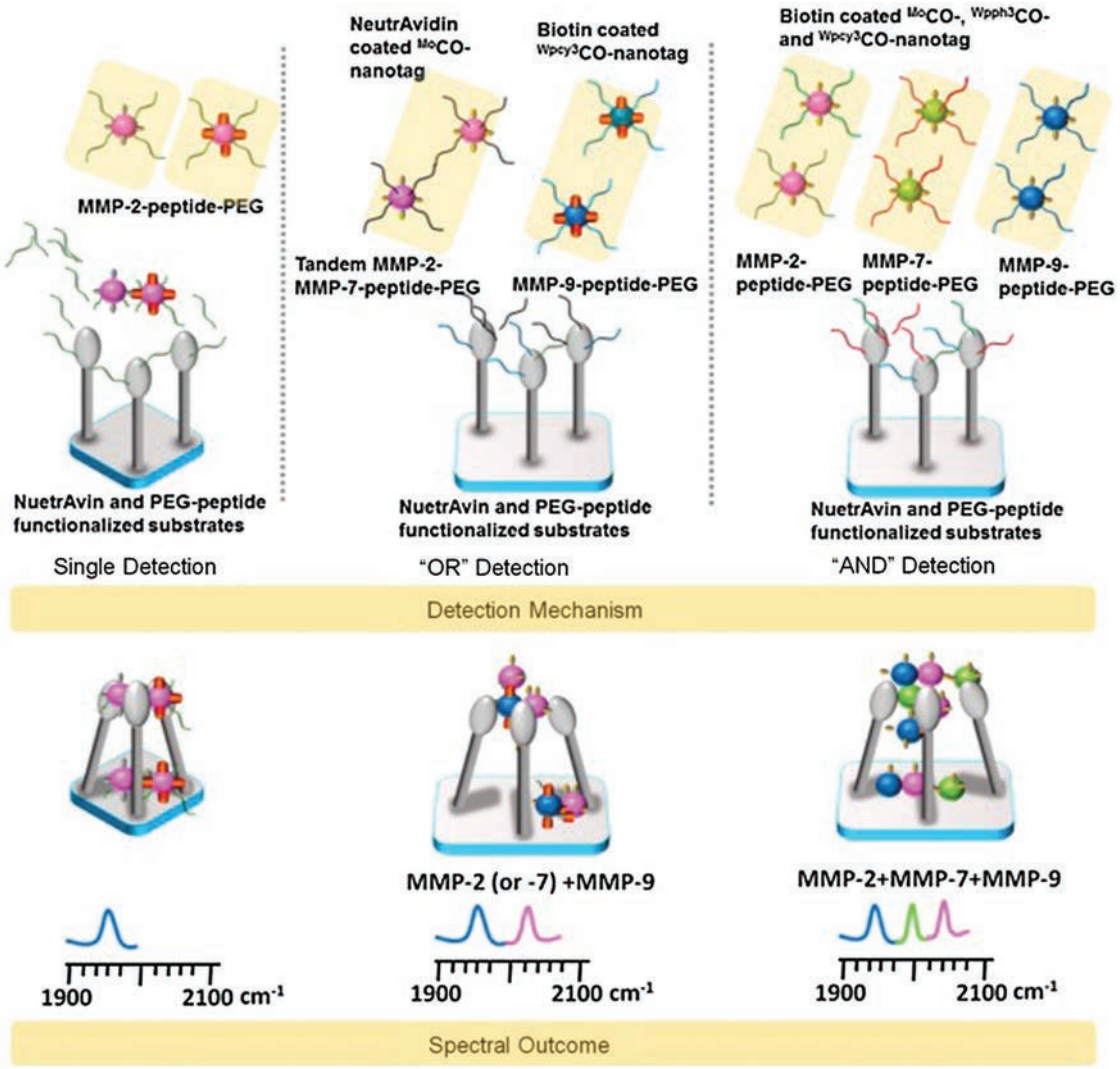

Figure 7. **Schematic of the mechanism for logical detection of MMPs with a nanopillar chip. Reprinted with permission from [153], Gong, T., et al., 2017. Optical interference-free surface-enhanced raman scattering CO-nanotags for logical multiplex detection of vascular disease-related biomarkers. *ACS Nano*, *11*(3), pp.3365–3375. Copyright@American Chemical Society.**

detection via sensing monodisperse iron oxide nanoparticles' (IONPs) magnetic relaxation. IONPs were first functionalized with NeutrAvidin and then linked by peptides, resulting in NP aggregates. These modifications caused changes in the magnetic signals. After the peptide linkers were cleaved by MMP-2, redispersing the IONPs exhibited magnetic responses close to the preaggregation state, which were applied to detect MMP-2 activity [156]. In a proposed strategy by Zhu et al., they constructed a magnetic nanoprobe, Fe_3O_4-pep-Gd, which was composed of Fe_3O_4 NPs, MMP-2 specific peptide linkers, and Gd chelates. Superparamagnetic Fe_3O_4 can hinder the longitudinal relaxation effect (T_1 relaxivity) of the connected Gd chelates once within an external magnetic field. In the case of cleavage of the peptide by MMP-2, the system releases Gd chelates, accompanied by T_1 contrast enhancement. By using diverse Gd chelates linked to one single peptide, the nanoconjugates could detect MMP-2 at a high sensitivity (down to 0.5 nM). The as-synthesized Fe_3O_4-pep-Gd nanoprobes were also utilized to sense MMP-2 under the levels of cells, as well as *in vivo* [157]. Additionally, by introducing a fluorescent dye as a reporter, Schuerle et al. designed magnetically actuated protease sensors (MAPS) for the detection of MMPs. The MAPS were constructed by co-encapsulating MNPs and peptide substrates functionalized with biotin and Cy7 dye into thermosensitive liposomes. When exposed to local alternating magnetic fields, the peptide linkers were released through the liposome assembly to the TME. Then, the overexpressed MMP-2 at the tumor site could cleave the peptide, resulting in cleaved Cy7 dye-linked reporters after isolation using streptavidin-coated beads (Fig. 8(a)). In this case, measurements of the cleaved reporters could be accomplished using the intensity of Cy7, which was used

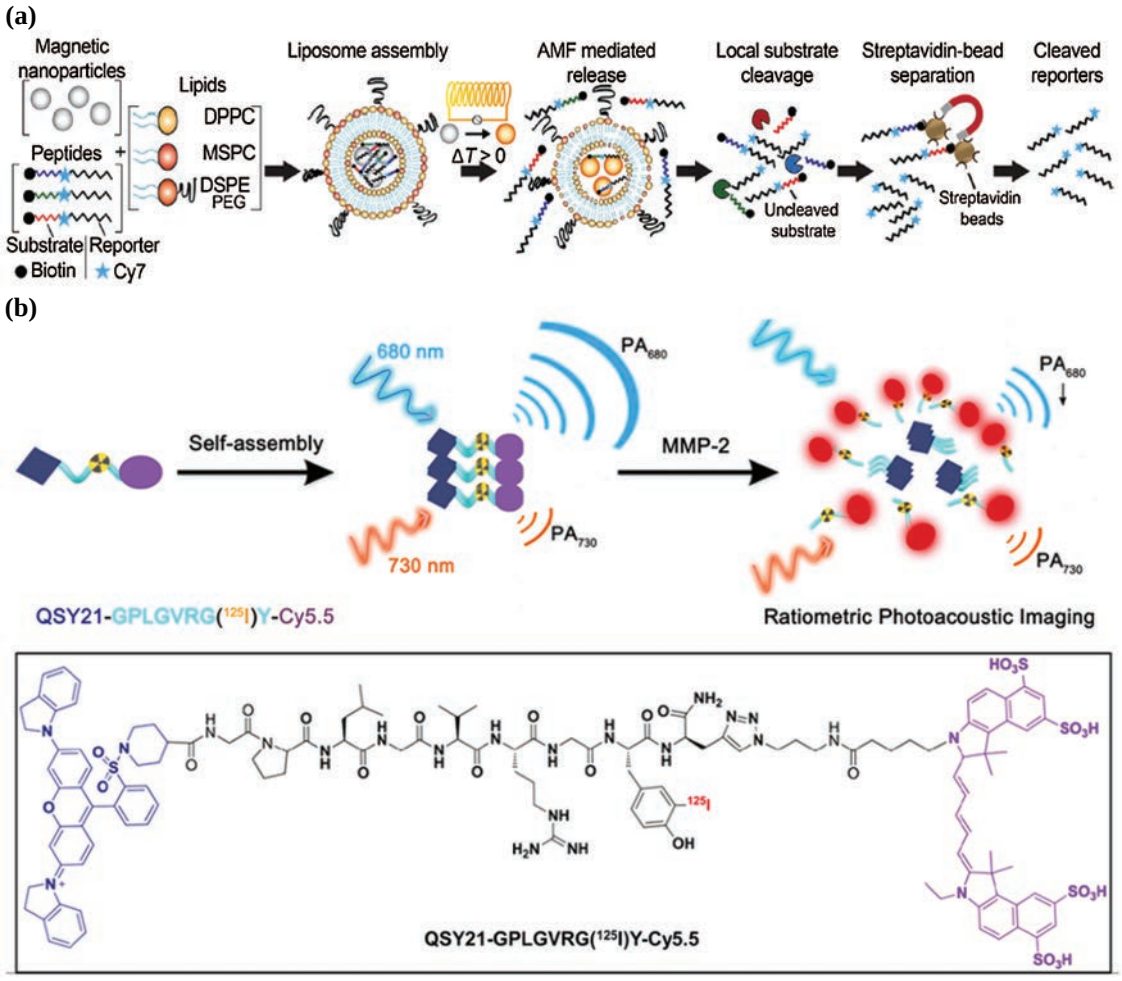

Figure 8. **(a) Construction strategy and schematic illustration of a magnetic operated protease probe. The liposomes, which contain the lipids DPPC, MSPC, and DPSE-PEG, were packaged with MNPs and synthetic peptides. As a urinary reporter, these peptide substrates were conjugated with a near-IR dye Cy7 and an N-terminal biotin. Reprinted with permission from [158], Schuerle, S., et al., 2016. Magnetically actuated protease sensors for in vivo tumor profiling. *Nano Letters*, *16*(10), pp.6303–6310. Copyright@American Chemical Society. (b) A probe for non-invasively detecting MMP-2 activity via fluorescence/photoacoustic imaging. Reprinted with permission from [161], Yin, L., et al., 2019. Quantitatively visualizing tumor-related protease activity in vivo using a ratiometric photoacoustic probe. *Journal of the American Chemical Society*, *141*(7), pp.3265–3273. Copyright@American Chemical Society.**

to monitor the activity of MMP-2. This magnetic nanosensor was successfully applied to sensor different MMPs in two types of xenograft mouse models [158].

Photoacoustic Imaging Nanoprobes

The photoacoustic (PA) effect is derivative from the acoustic wave yielding optical excited biomolecules, which allows in-depth imaging of biological tissues with minimal signal loss *in vivo*. Recently, enzyme-selective PA imaging probes have been widely investigated for enzyme detection in cells and *in vivo*. Typically, an activatable PA imaging nanoprobe is designed using various nanomaterials, including CuS-NPs and Au nanostructures as substrates, based on the reaction mechanism of proteolytic processing with enzyme or enzymatic cleavage capability [142]. Based on a cleavage and retention strategy, Yang et al. reported an activatable PA nanoprobe (CuS-peptide-BHQ-3) via the conjugation of a specific quencher 3 (BHQ3) to CuS-NPs through a MMP-cleavable peptide liker. The constructed nanoprobe could be exhibited by two optical wavelengths at 680 nm and 930 nm to obtain PA signals. When delivered into tumor lesions *in vivo*, overexpressed MMPs could cleave the peptide linker and could release BHQ3 from the probe CuS-NPs. After the clearance of BHQ3 by the tumor-specific enzyme, tumor lesions retained CuS-NPs, inducing a constant PA signal at 930 nm. Thus, the changes in PA signals with ratios at 680 nm/930 nm could be used for the detection of MMP activity *in vivo* [159]. In another examination, Zhang et al. used a different strategy to construct a PA imaging probe according to the enzyme-triggered self-assembly of nanostructures. Due to the assembly prompt

retention effects, beneficial PA imaging signals could be observed in the presence of a certain specific enzyme, which could contribute to enhanced diagnosis and therapy of tumors [160]. Recently, Yin et al. reported quantitative visualization of MMP-2 activity utilizing a ratiometric PA nanoprobe *in vivo*. The PA imaging probe consisted of the near-infrared dye Cy5.5 and a fluorescence quencher QSY21, that were conjugated through a peptide specific to MMP-2. After cleaving the peptide linker by MMP-2, the recovered fluorescence signal was related to the level of MMP-2. Additionally, the nanoprobe exhibited distinct PA signals that were MMP-2 level dependent at 680 nm and constant at 730 nm (Fig. 8(b)). This PA signal change enabled MMP-2 detection by both PA signals and fluorescence in cells and *in vitro*. Benefiting from its deep tissue penetration capability, ratiometric PA imaging was achieved for the quantitative MMP-2 expression detection *in vivo* [161].

Enzyme-Triggered Drug Release for Targeted Tumor Therapy

For tumor treatment, the specificity and efficiency in delivering therapeutic compounds to targets are critical. Enzyme overexpression in a tumor environment provides a chance for the development of enzyme-triggered DDSs for potential site-specific antitumor therapies [141]. In recent years, by creating self-assembling systems that mimic nature, various self-assembled nanomaterials have shown enormous potential [162, 163]. For instance, supramolecular self-assembly, e.g., β-sheet-forming peptides, have been reported for the development of DDSs. Kalafatovic et al. designed a supramolecular nano-assembly system from a peptide structure and MMP-9 substrate. The short sheet-forming peptides could form micelles with a hydrophobic pocket to encapsulate the anticancer drug DOX and then integrate with the MMP-9 substrate. When applied to a tumor-bearing mouse model, the formation of DOX-containing fibers was triggered upon hydrolysis of the nanocomposite by MMP-9 at the tumor site, which exhibited better tumor treatment efficacy than DOX alone. This study demonstrated the advantage of using an enzyme-triggered drug release system for targeted tumor therapy [164]. Supramolecular self-assembly was formed based on a nucleation mechanism, which is a rate-limiting process. To improve the tumor-specific accumulation of drugs via kinetic control, Cheng et al. designed an autocatalytic morphology transformation nanoassembly system that was self-assembled from a nanocomposite (CPT-LFPR) composed of a drug unit, β-sheet-forming peptides, an enzyme-cleavable peptide linkage, a hydrophilic unit, and a targeting unit (Fig. 9(a)) [137]. The enzyme-cleavable linker can be specifically degraded by cathepsin B, which is a critical lysosomal protease that is high expressed in different cancer cells [165]. In the presence of cathepsin B, the peptide linkers on the nanoassembly, CPT-LFPR, were cleaved. Accompanied by the shedding of the hydrophilic shell, the NPs were reorganized into β-sheet fibrous structures that served as "seeds" to accelerate the morphology transformation of NPs to fibrous prodrug structures (Fig. 9(b)). By administrating fluorescently labeled CPT-LFPR into Hela tumor-bearing mice, the targeted retention of fibrous prodrugs in the tumor lesions *in vivo* after multiple administrations and the autocatalytic growth of the fibrils were clearly monitored (Fig. 9(c)). Additionally, the released drug exhibited significant tumor growth inhibition, demonstrating the efficacy of the developed morphology transformation strategy and its potential for targeted delivery of therapeutic drugs [137].

Enzyme-Responsive Nanomaterials for Imaging-Guided Synergistic Therapy

Imaging-guided therapies play increasingly important roles in cancer treatment due to their abilities to improve treatment efficiency and specificity [166]. The construction of an enzyme-activatable theranostic system that can enable imaging and targeted drug delivery has been extremely desirable for the precise diagnosis of cancer and effective therapy. Hu et al. developed the strategy of a FRET-based theranostic nanoprobe that integrated gold nanorods (AuNRs) into a PS of pyropheophorbide-a (PPa) via a MMP2-responsive peptide linker (CGPLGVRGK) (Fig. 10(a)). In that study, AuNRs were applied as not only the nanocarrier and fluorescent quencher of PS but also as a photothermal reagent. Additionally, PS held a post in the reagent for both fluorescence imaging and PDT, owing to its favorable optical properties. Owing to the FRET effect between AuNRs and PSs, the nanoprobe was not fluorescent. After it was taken up by the MMP2 enzyme-overexpressed tumor cells, the nanoprobe was cleaved by the MMP2 enzyme at the peptide linker, resulting in switched on of the fluorescence in cells and $^1O_2$ production of PPa. Thus, imaging-guided synergistically activated photothermal therapy were achieved for the efficient killing of cancer cells, which indicated the successful application of enzyme-responsive theranostic nanoprobes for molecular imaging and site-specific cancer treatment [167]. Enzyme-responsive therapy enables site-specific control of treatment and provides promising tools for imaging-guided synergistic treatment. To improve the signal-to-noise ratios and avoid possible "false positive" outcomes by single stimulus-responsive therapies, Yan et al. developed a dual activatable nanoprobe with the capability of stimulus-response and reversibility for tumor-imaging and fluorescence-guided PTT. The nanoprobe was composed of AuNRs, a fluorescent dye asymmetric cyanine (Acy), and a MMP-cleavable peptide linker. The fabricated nanoprobe, Pep-Acy/Glu@AuNR, was non-fluorescent owing to the FRET effect and base form of the Acy. Upon exposure to MMP-13 in an acidic microenvironment, the detached Acy was changed to its acidic

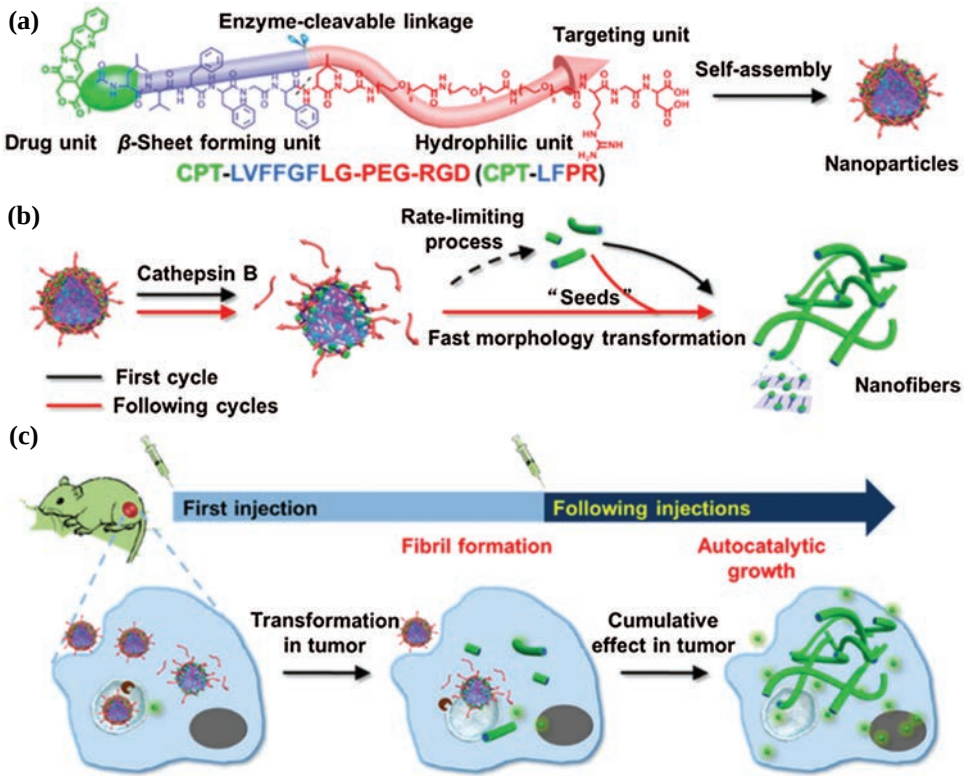

Figure 9. **Strategies of enzyme-triggered nanofiber morphology transformation and autocatalytic growth. (a) Self-assembly process of CPT-LFPR. (b) According to the autocatalytic growth mechanism, fibrils promote the transformation of nanofibers. (c) Intravenous NPs illustrates the cumulative effects on fiber prodrugs. Reprinted with permission from [137], Cheng, D.B., et al., 2019. Autocatalytic morphology transformation platform for targeted drug accumulation. *Journal of the American Chemical Society*, *141*(10), pp.4406–4411. Copyright@American Chemical Society.**

form, resulting in fluorescence recovery. Additionally, the nanoprobe, Pep-Acy/Glu@AuNR, could be reversibly activated with a pH change. Combined with the photothermal effect of AuNRs and Acy, the dual stimuli-activatable theranostic nanocomposite was smoothly employed to the tumor-targeting fluorescence imaging-guided phototherapy using tumor-bearing mice models [168].

For imaging-guided theranostic systems, multimodal imaging approaches have drawn considerable attention owing to the diagnostic information obtained from several techniques. A gadolinium (Gd)-hybridized plasmonic gold nanocomposite, which could achieve HAase-responsive drug release, had been designed by Wang et al. for chemotherapeutic drug delivery to cancer lesions under the guidance of highly sensitive multimodal imaging [169]. The same group further designed the fabrication of HA-functionalized MoS_2 assisted by polyethyleneimine (PEI) as a multifunctional nanocomposite (MoS_2-PEI-HA) for chemotherapy drug DOX delivery and multimodal imaging-guided tumor therapy. Then, 2D transitional metal dichalogenides, e.g., MoS_2, which has a strong NIR photothermal conversion ability to ablate cancer cells, was applied as the substrate of the nanoprobe. HA could specifically discriminate the CD44 receptor on tumor cells and be degraded by the protease HAase, which was abundant in the TME. The as-prepared nanoprobe MoS_2-PEI-HA exhibited multi-stimulus-responsiveness according to the HAse, pH, and NIR laser, inducing accelerated DOX release in tumor cells guided by real-time positron emission tomography imaging (Fig. 10(b)) [170].

OXIDATION-REDUCTION-REGULATED ACTIVATABLE NANOSYSTEM

ROS are the main species generated by oxidative stress, and they play crucial roles in tumor occurrence, progression, and recurrence [171]. The redox status maintains a relative balance in normal cells. Once this balance is broken, oxidative stress will occur, leading to a series of diseases, including diabetes, aging, fat peroxidation disorder, neurodegeneration, and cancer. Glutathione (GSH), a tripeptide molecule widely presented in cells, is a natural non-enzymatic antioxidant. GSH is very important in the antioxidant defense system of organisms, preventing oxidative stress from destroying the tissue and organs [172]. A change in the ratio of GSH/GSSG is the main dynamic indicator that reflects the redox status. Various studies have reported that elevated ROS and GSH levels were found in tumor cells in comparison with normal cells, which caused tumor cells to have a

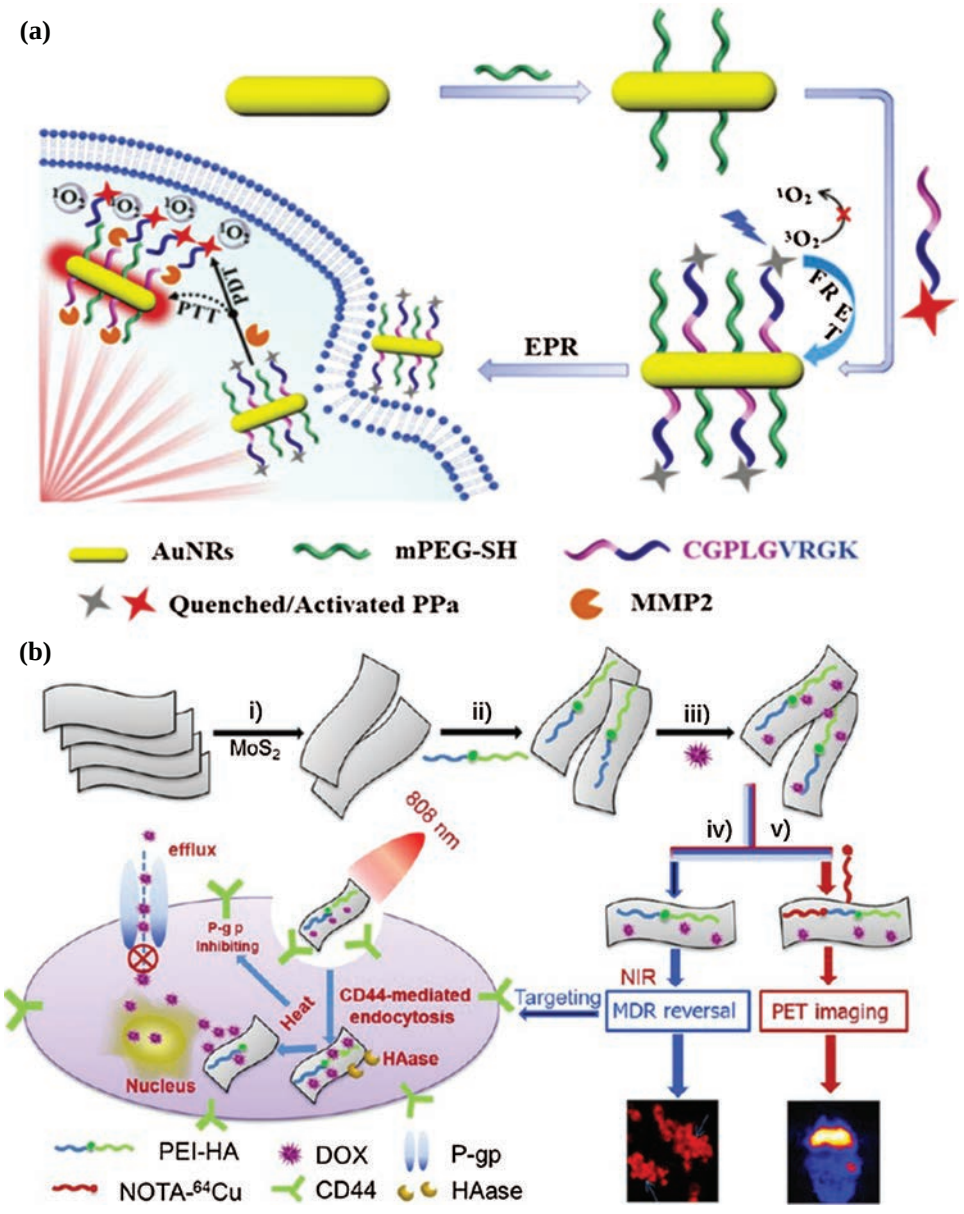

Figure 10. **(a) The design and synthesis of tumor therapeutic nanoprobes based on the MMP2 activation platform, as well as the strategy for precise tumor-targeting and lesion-specific phototherapy. Reprinted with permission from [167], Hu, B., et al., 2019. Activatable smart nanoprobe for sensitive endogenous MMP2 detection and fluorescence imaging-guided phototherapies. *Inorganic Chemistry Frontiers*, *6*(3), pp.820–828. Copyright@Royal Society of Chemistry. (b) MoS_2-PEI-HA nanosheets serve as a multifunctional platform for PET imaging-guided MCF-7-ADR cell targeting and multiple stimulus-response therapy. (i and ii) An improved liquid lift-off process to prepare single-layer MoS2 nanosheets, which modified with HA. (iii) Illustration of the loading process for acquiring DOX@MoS2-PEI-HA. (iv) MoS2-PEI-HA nanosheets utilizes the inhibition of P-gp protein to achieve active DOX transmission against CD44 and MDR reversal. (v) After functionalized with NOTA-64Cu for PET imaging. Reprinted with permission from [170], Dong, X., et al., 2018. Intelligent MoS_2 nanotheranostic for targeted and enzyme-/pH-/NIR-Responsive drug delivery to overcome cancer chemotherapy resistance guided by PET imaging. *ACS Applied Materials & Interfaces*, *10*(4), pp.4271–4284. Copyright@American Chemical Society.**

higher redox potential [173]. Such a large concentration difference allows modified drugs with redox response sites to be potentially applied in the design of a series of redox-responsive nanomedicines and gene delivery systems [174, 175]. In this section, assembly-disassembly-based DDSs via redox regulation will be discussed.

ROS-Responsive Drug Delivery Nanosystems

Due to low solubility and high toxicity, the application of tumor-targeted drugs has been greatly restricted. NP DDSs have showed great potential for solving these issues. Because ROS are overexpressed tenfold in the TME compared with normal cells, various ROS-responsive prodrugs

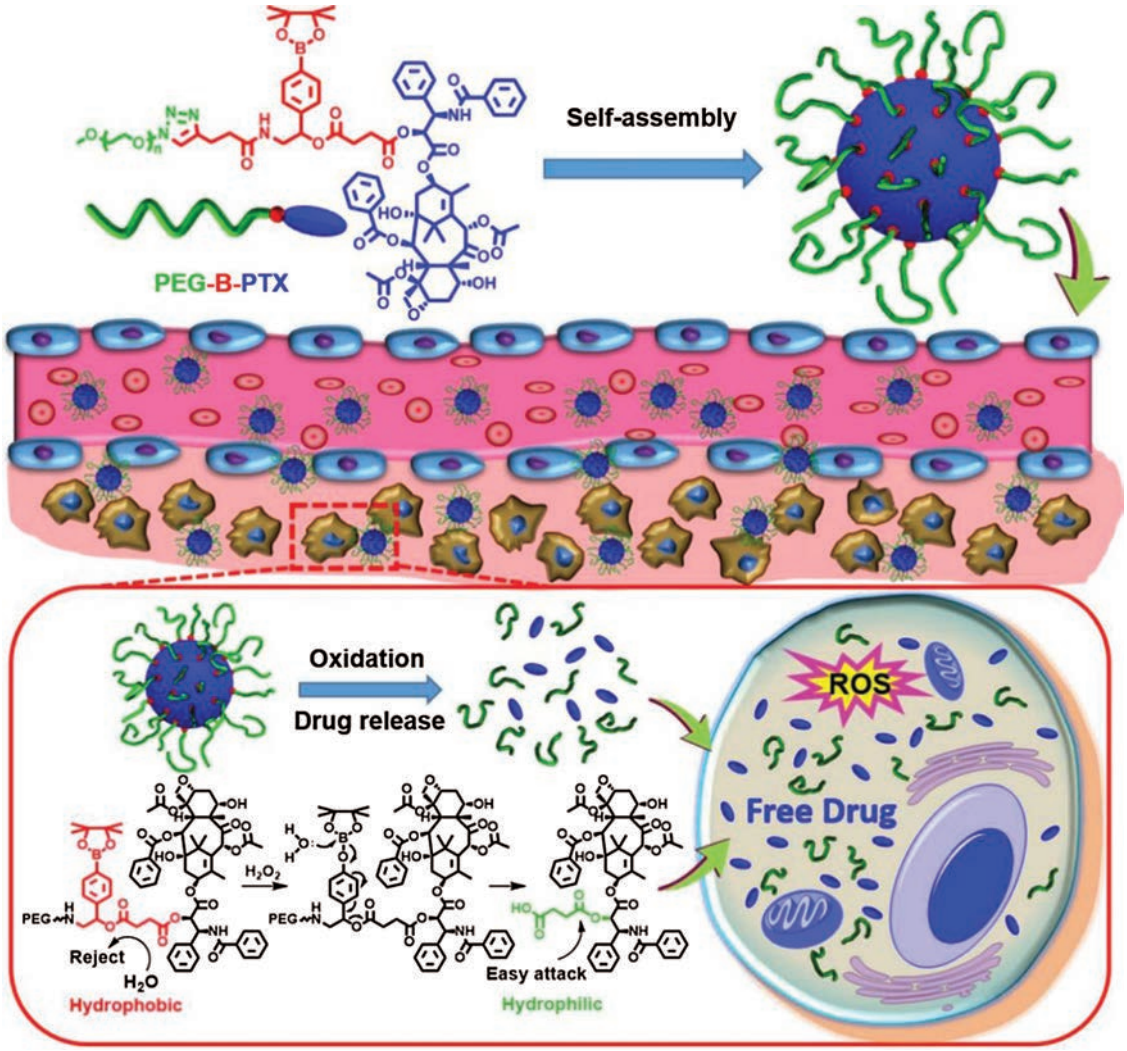

Figure 11. **Micelle formation and application of the PTX-based prodrug. PEG-B-PTX was activated by H_2O_2 in tumor microenvironment and produced the PTX drug release for tumor therapy. Reprinted with permission from [185], Dong, C., et al., 2020. Self-assembly of oxidation-responsive polyethylene glycol-paclitaxel prodrug for cancer chemotherapy. *Journal of Controlled Release*, *321*, pp.529–539. Copyright@Elsevier.**

with high water solubility and low toxicity have been developed recently [176–179]. Here, we highlight a few representative examples to illustrate the application of ROS-responsive drug delivery nanosystems.

Arylboronic esters are easily oxidized by H_2O_2 to phenol with an elimination reaction in the TME; thus, they are widely used in the design of tumor DDSs [180–182]. For example, Luo et al. constructed a drug delivery nanosystem, namely PPHC NPs, consisting of PEG and PPH based on coordination interactions between curcumin and boronic acid [183]. The nanosystem could effectively improve the stability of Cur in the physiological pH range. *In vitro* experiments showed that PPHC NPs were destroyed after incubation of H_2O_2 and thus released Cur. When A549 cells were treated with PPHC NPs, they were found to have a stronger anti-proliferation effect in comparison with only Cur-treated cells. Using this chemistry, Zhang et al. designed three phenylboronic ester-based 1,8-naphthalimide copolymer NPs by atom transfer radical polymerization wherein DOX was loaded into the cavity of NPs [184]. In the presence of H_2O_2, release of 100% DOX from MF1 NPs was achieved in 24 h, accompanied by ratiometric fluorescence signal outputs. The MF1 NPs could enter A549 cells via the endocytosis pathway and released DOX, which was slowly triggered by endogenous H_2O_2 within the cancer cells. The process of H_2O_2-triggered DOX release in the cells was tracked *in situ* by fluorescence ratio signal changes. Unfortunately, the MF1 drug delivery system is not sensitive to H_2O_2 levels in the cancer cells, which has limited its use as a nanomedicine for cancer therapy. More recently, Dong et al. constructed a PEG-B-PTX prodrug by introducing an arylboronic ester linker between PEG and paclitaxel (Fig. 11) [185]. This prodrug had the characteristics of an amphiphilic polymer

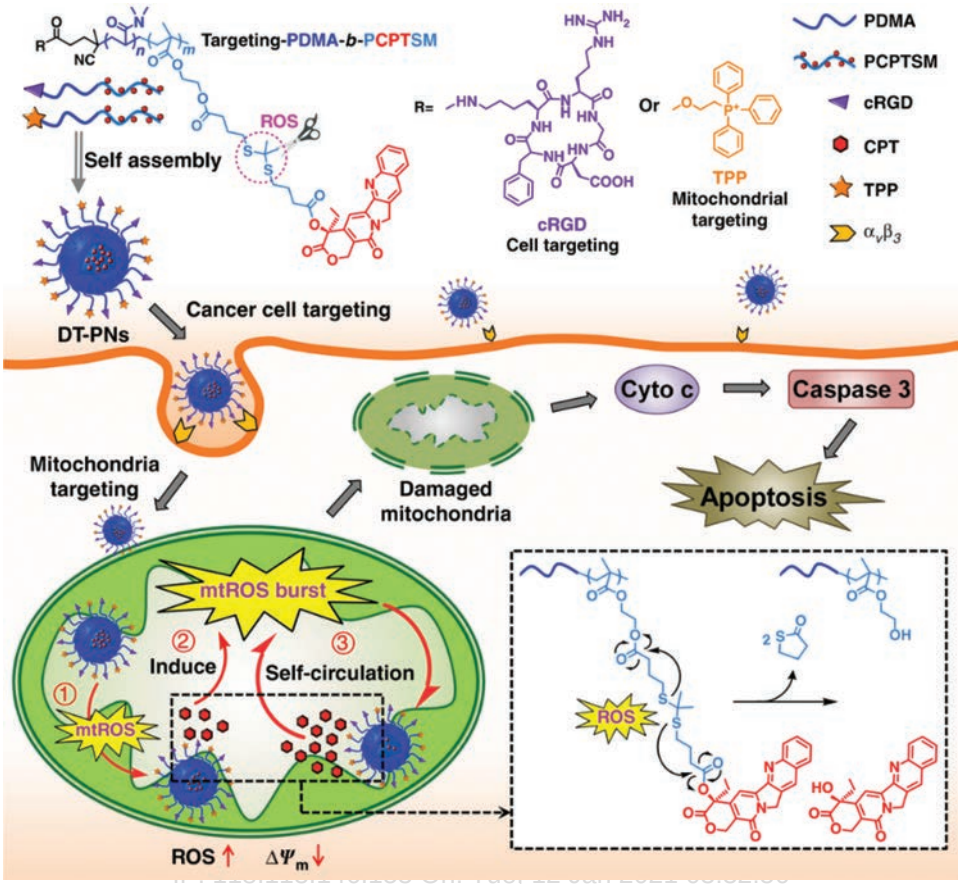

Figure 12. **The formation and application of prodrug nanoplatform DT-PNs. DT-PNs were composed of cRGD-PDMA-b-PCPTSM, TPP-PDMA-b-PCPTSM, and CPT. Reprinted with permission from [187], Zhang, W., et al., 2019. Mitochondria-specific drug release and reactive oxygen species burst induced by polyprodrug nanoreactors can enhance chemotherapy. *Nature Communications*, *10*(1), pp.1–14. Copyright@Nature Publishing Group.**

and enabled self-assemble to form micelles with a size of approximately 50 nm. In the absence of H_2O_2, the micelles were stable, and only 5% PTX was released after 96 h. Upon H_2O_2 stimulation, the arylboronic ester in the micelles was first oxidized and then hydrolyzed to release PTX. The pharmacokinetics results demonstrated that PEG-B-PTX micelles had a longer blood circulation duration. The PEG-B-PTX micelles could quickly respond to the excessive production of H_2O_2 in the tumor to release PTX. The antitumor efficiency of the PEG-B-PTX micelles versus Taxol was found to be significantly enhanced against breast and human glioma cancer cells.

Different from the arylboronic esters-based prodrug, Liu and coworkers developed an amphiphilic polymer self-assembly system containing a selenide and phosphate moiety, which was applied as a nanoplatform for drug delivery [186]. The designed polymer P1 appeared to self-assemble into a core/shell structure in water owing to the amphiphilic branched backbone. Upon H_2O_2 treatment, the selenide moiety was easily oxidized into selenone, which means the hydrophobic segments of P1 were converted to hydrophilic groups, thus causing disassembly. Based on the properties of P1, DOX-loaded P1 micelles were constructed. The results of *in vitro* anticancer experiments revealed that the DOX-loaded P1 micelles enabled quick release of DOX under stimulation of endogenous H_2O_2, and it had a good anti-proliferative effect on cancer cells.

Although several ROS-responsive DDSs have been reported to treat tumors, insufficient levels of endogenous ROS reduce the therapeutic effect to some extent. To address this problem, Zhang et al. presented a ROS-responsive self-circulation prodrug (DT-PNs) with dual targeting of mitochondria and tumor cells. CPT was grafted into DT-PNs via a ROS-cleavable thioketal linker (Fig. 12). In this system, DT-PNs were first targeted to cancer cells, and then, CPT was released from the DT-PNs under the stimulation of endogenous mtROS in the TME. Finally, CPT, a respiratory inhibitor, could further induce the mtROS to burst to enhance cancer therapy. Detailed *in vivo* results demonstrated DT-PNs showed no obvious toxicity or side effects in mice. Treatment with DT-PNs significantly inhibited tumor growth and regression [187]. Using a similar concept, Park et al. reported ROS-triggered self-accelerating drug delivery NPs (PTS-DP), where DOX and the PS, pheophorbide A (PhA), were encapsulated

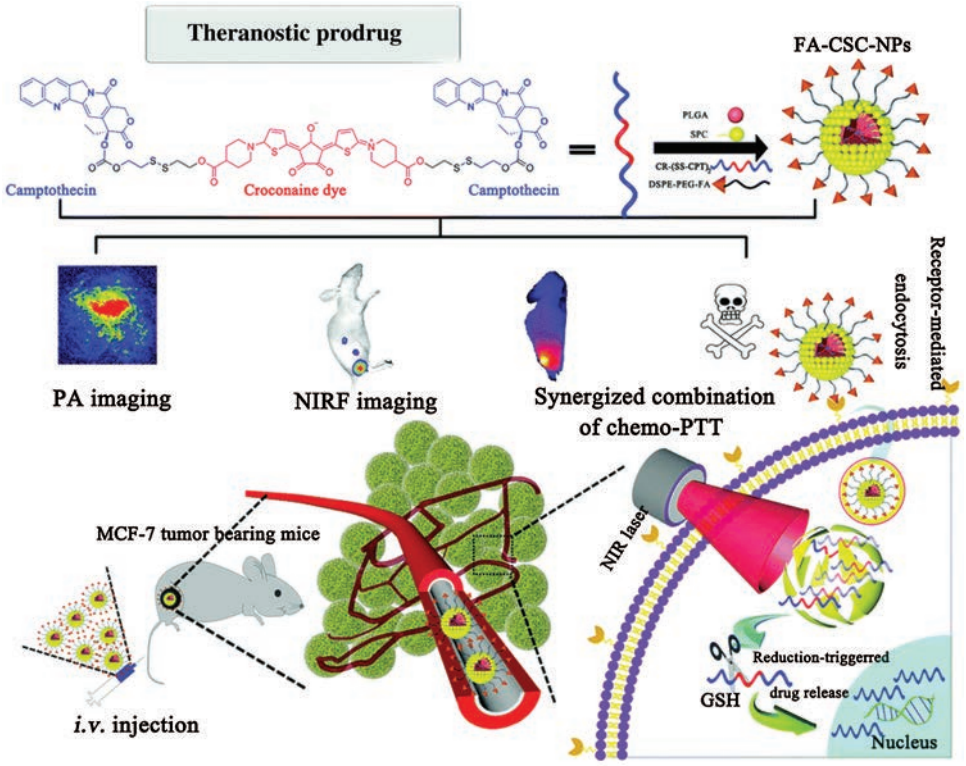

Figure 13. **CPT-based GSH-responsive polydrug (FA-CSC-NPs) for image-guided combinational therapy. Reprinted with permission from [194], Yu, F., et al., 2018. Redox-responsive dual chemophotothermal therapeutic nanomedicine for imaging-guided combinational therapy. *Journal of Materials Chemistry B*, *6*(33), pp.5362–5367. Copyright@Royal Society of Chemistry.**

in the PEG-stearamine-containing ROS-activatable thioketal linkage [188]. After uptake into the cancer cells, the thioketal linkage of PTS-DP was activated to release DOX and PhA owing to endogenous ROS production. Upon irradiating with a NIR laser, singlet oxygen was produced by PhA, which in turn further accelerated the production of ROS in the tumor region. This synergistic effect provided PTS-DP with a potent ability to inhibit tumor growth.

GSH-Responsive Drug Delivery Nanosystems

In the extracellular matrix, the GSH concentration is 2–20 μM, whereas the concentration in normal cells is 2–20 mM. The level of GSH in tumor tissue is approximately four times higher than in normal tissue. Thus, the disulfide bond can be easily reduced in the tumor, and modified drugs with disulfide have been applied to design a large amount of redox-responsive nanomedicines and gene delivery platforms [189–191]. The designed delivery platforms can release the free drugs under stimulation of endogenous GSH in a tumor tissue microenvironment, thus improving drug efficacy.

Some GSH-responsive drug delivery nanosystems have been reported. For instance, Liu et al. recently prepared an amphiphilic copolymer, namely H40-star-PLA-SS-PEP, that was composed of a redox-sensitive disulfide linkage, the drug delivery carrier, H40, and biodegradable PLA [192]. The copolymer could self-assemble to form a core–shell structure in aqueous solution with an average size of 70 nm. DOX release from DOX-loaded H40-star-PLA-SS-PEP in the cells was also examined. Blank DOX-loaded H40-star-PLA-SS-PEP displayed low cytotoxicity to the cells, which was mainly due to the low concentration of DOX in the culture medium. Upon pretreatment with 0.1 mM BSO (an inhibitor of GSH), DOX-loaded H40-star-PLA-SS-PEP displayed lower cytotoxicity to the cells. With the existence of GSH-OEt, DOX was rapidly released from the micelles and provided enhanced cytotoxicity to tumor cells. Using similar design strategies, Xu et al. designed and synthesized an amphiphilic mitochondria-targeting prodrug DCT that comprised PEG, triphenylphosphonium bromide (TPP), dextran (DEX), and disulfide linkage CPT [193]. TPP decorated in the copolymer chain led to the depolarization of the mitochondria potential and delivered DCT micelles into the mitochondria. The results revealed DCT only released a small quantity of CPT in the blood circulation. However, exposure to a highly reduced tumor microenvironment and CPT release from DCT was significantly accelerated due to the cleavage of disulfide linkages. Mouse model experiments confirmed that DCT micelles could not only effectively inhibit tumors but also showed no obvious side effects, such as inflammation or infection.

Similarly, Yu et al. designed another CPT-based GSH-responsive polydrug (FA-CSC-NPs) for imaging-guided

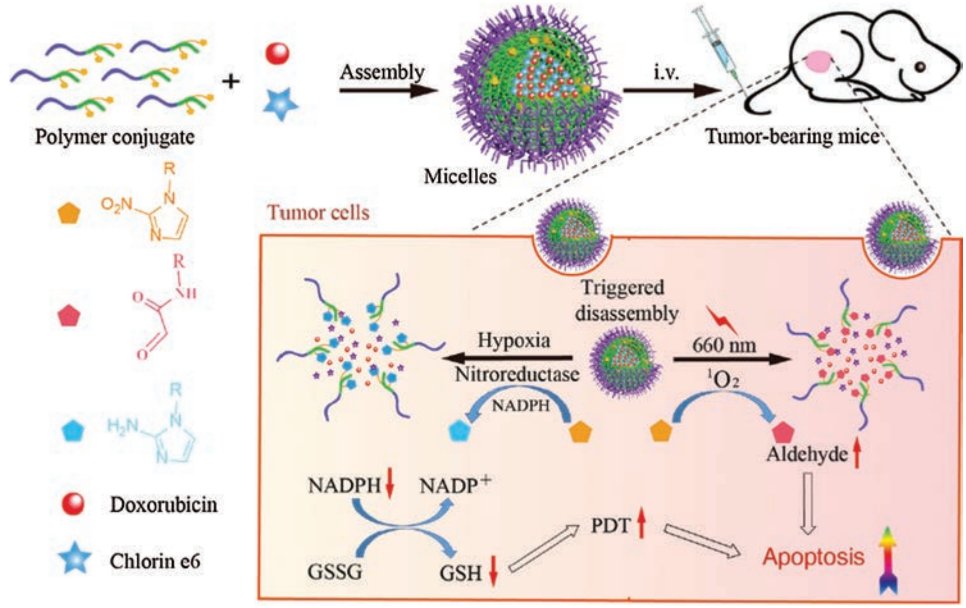

Figure 14. Construction of dually responsive nanomicelles for effective delivery of Ce6 and DOX as the photosensitizer and chemodrug, respectively, and controllable release of cargos in a tumor-bearing mice model. Reprinted with permission from [211], Deng, J., et al., 2019. Hypoxia- and singlet oxygen-responsive chemo-photodynamic micelles featured with glutathione depletion and aldehyde production. *Biomaterials Science*, *7*(1), pp.429–441. Copyright@Royal Society of Chemistry.

combinational therapy in which CPT linked with a near-infrared croconaine fluorophore via disulfide bonding was encapsulated into folate modified PLGA NPs (Fig. 13) [194]. After they were triggered by GSH, CPT and CR underwent rapid release from FA-CSC-NPs in tumor cells due to the cleavage of the disulfide linkage. Upon NIR laser irradiation, CR release from the NPs was capable of converting light into heat. Interestingly, the controlled release process of CPT was accelerated. It was mainly due to the fast-diffusion of CPT and increased cleavage rate of the disulfide bond induced by the heat generated from CR. FA-CSC-NPs had excellent tumor-targeting ability. *In vivo* experimental results also demonstrated that FA-CSC-NPs could significantly inhibit tumor growth, and the tumor was completely cleared within 14 days.

Unlike disulfide linkage, dithiomaleimide was also employed to construct DDSs [195, 196]. For instance, Wang et al. designed and synthesized a novel GSH-responsive dithiomaleimide-based prodrug ((CPT)2-Mal-PEG1k) wherein CPT-thiols were conjugated to PEG via a maleimide linker [196]. The drug loading capacity of (CPT)2-Mal-PEG1k reached 60%, and the release of CPT exceeded 95% after treatment with 5 mM GSH. Additionally, in the presence of GSH, the ratios of fluorescence intensities (I_{438}/I_{550}) gradually increased due to the GSH-triggered release of CPT. An *in vitro* anticancer experiment revealed that (CPT)2-Mal-PEG1k possessed excellent proliferation inhibition capability. The results demonstrated that (CPT)2-Mal-PEG1k could be a preferable drug delivery candidate for cancer treatment.

CONSTRUCTION OF EFFICIENT THERAPEUTIC NANOMATERIALS BASED ON A TUMOR-SPECIFIC HYPOXIC MICROENVIRONMENT

Compared with normal tissues, more than 60% of solid tumor tissues are found to be hypoxic, which has been a representative hallmark of the TME [197–199]. The reason for the hypoxia is that the oxygen supply from the blood cannot meet the consumption requirements of solid tumors, where the abnormally vigorous cell growth, disorganized vasculature, and short diffusion distance of oxygen in the tumor tissue together cause this pathological phenomenon. In general, hypoxia is a key regulator of a tumor that can usually induce malignant aggressiveness, progression, and metastasis [200]. Moreover, the hypoxic environment inside the tumor tissues also significantly influences multiple cancer therapies, such as chemotherapy, PDT, radiotherapy (RT), and sonodynamic therapy, either directly or indirectly [201]. Although hypoxia is normally regarded as an adverse prognostic indicator for cancer treatment, the unique biological features of hypoxic cancer tissues enable them to act as a specific target in fighting against cancer [202–204]. Numerous hypoxia-responsive prodrugs and relevant nanosystems have been developed to solve this issue [205]. In this chapter, discussions are mainly focused on the functional nanomaterials that utilize the hypoxic microenvironment as an advantageous stimulus factor to facilitate cargo liberation or activated theranostics for effective cancer treatment.

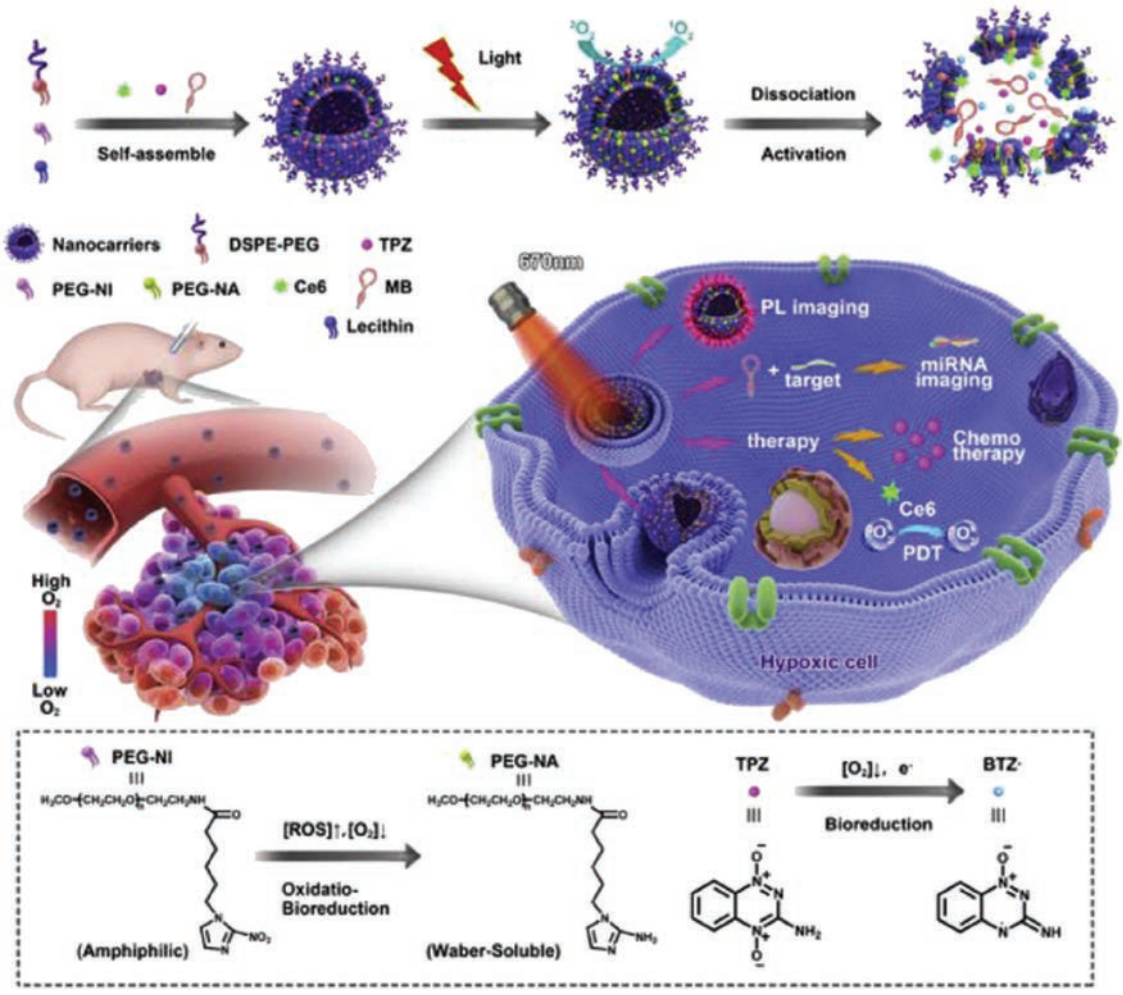

Figure 15. **Construction of Lip/Ce6/TPZ NPs and hypoxia-activated PDT and combined chemotherapy to fight against cancer upon light irritation. Reprinted with permission from [216], Zhang, K., et al., 2018. Light-triggered theranostic liposomes for tumor diagnosis and combined photodynamic and hypoxia-activated prodrug therapy. *Biomaterials*, *185*, pp.301–309. Copyright@Elsevier.**

Nanomaterials Specific to Hypoxia-Responsive Cargo Liberation

Current therapeutic fields have undergone unprecedented evolution and are largely focused on "personalized medicines" instead of "one drug for all [206, 207]." This evolution reflects improvements toward a new paradigm regarded as the therapeutic ideal. The development of nanomedicine intends to promote the efficacy, accuracy, and safety for satisfactory diagnosis and therapy of cancer via utilizing the prominent characteristics of designed nanomaterials. For NPs that are sensitive to the TME, they can not only target tumors by both the active recognition and EPR effect but also prolong the retention time of drugs [208]. Inspired by the specific hypoxic TME, various functional nanomaterials have been designed and constructed to achieve tumor-targeted delivery and controllable cargo release, including anticancer prodrugs and/or therapeutic agents, which show great potential for addressing the dilemma of on-demand liberation at cancer sites [209, 210].

Delivery of combinational drugs/therapeutics has been an effective method for tumor management. Polymeric micelles, which usually serve as drug delivery vehicles, can be designed with excellent targeting ability and good stability to facilitate combinational cargo delivery. Recently, Zhao and colleagues reported a multifunctional nanosystem for a dual stimulus-responsive combination of PDT and chemotherapy (Fig. 14) [211]. The micelles, composed of a nitroimidazole (NI)-based polymer, incorporated DOX and chlorin e6 (Ce6) as the chemodrug and photosensitizer, respectively. Under an hypoxia stimulus, the NI section could be bio-reduced and resulted in the disassembly of micelles, glutathione (GSH) depletion, and rapid payload release. Further laser irradiation led to collapse of the micelle, enhanced cargo liberation, and the production of aldehyde due to oxidation of NI by the Ce6-produced singlet oxygen. Fast drug release facilitated the

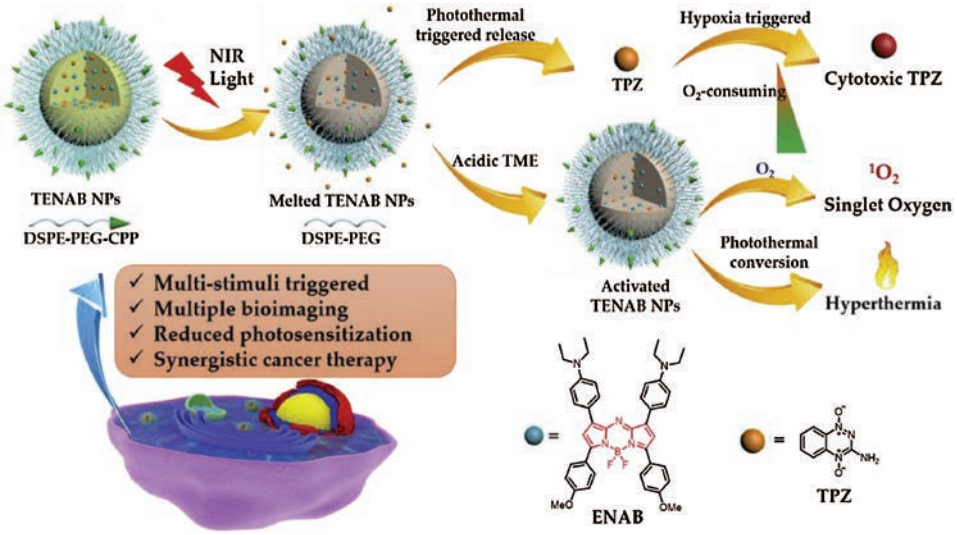

Figure 16. **Schematic illustration of TENAB NPs with multi-stimuli responsiveness for synergistic anticancer therapy. Reprinted with permission from [217], Chen, D., et al., 2019. Photothermal-pH-hypoxia responsive multifunctional nanoplatform for cancer photo-chemo therapy with negligible skin phototoxicity. *Biomaterials*, *221*, pp.1–11. Copyright@Elsevier.**

effective therapeutics; meanwhile, aldehyde production, and GSH depletion could provide supplementary action to boost the antitumor outcome of the co-delivery micelles. *In vitro* and *in vivo* experiments have demonstrated satisfactory efficacy in a 4T1 model. This work broadened the availability of traditional stimulus-responsive nanomaterials to provide both controlled release and a magnified antitumor effect.

Multifunctional Nanotheranostic System Combined with Hypoxia-Activated Therapy

The global increase in cancer diagnoses, combined with highly efficient phototherapies and traditional chemotherapies, has necessitated the discovery of novel drugs and delivery vehicles that regulate their anticancer effects via tumor-specific mechanisms. Developing effective imaging methods to monitor the therapy process of cancer and flow of drug molecules in cells is essential for evaluation of therapeutic efficacy and safety [212]. Moreover, multi-therapeutic synergistic treatment has an important effect on the treatment of hypoxic tumors compared with monotherapy [213, 214]. Recently, researchers successfully designed a variety of multifunctional nanotheranostic systems to achieve both early diagnosis and precise treatment.

A hypoxia microenvironment has been the main obstacle for effective PDT, which utilizes PS to produce ROS with the existence of O_2 and directly kill cancer cells. Fortunately, hypoxia-responsive chemotherapy integrated with PDT may serve as an alternative method for enhancing antitumor therapy [215]. Inspired by this, a hypoxia-responsive amphiphilic polymer-based theranostic liposome was developed, which incorporated Ce6 as PS, gene probe miRNA-155, and the hypoxia-activated prodrug tirapazamine (TPZ) for combined PDT-chemotherapy (Fig. 15) [216]. When the target was absent, the fluorescence of miRNA-155 was quenched as a result of the close distance between the labeled fluorescence dye and the quencher. Treatment of the target led to the separation of fluorescence dye from the quencher, which finally produced the detected fluorescence signal. Upon light irradiation, PDT mediated by Ce6 could induce severe hypoxia, leading to the disassembly of liposomes and activating the anticancer effect of TPZ, which could improve the cancer-killing efficiency. Simultaneously, the released gene probe provided a promising approach to differentiate the tumor cells from normal cells via detecting oncogenic intracellular biomarkers.

Apart from synergistic therapy activated by the hypoxia microenvironment, appropriate nanomaterials to achieve imaging-guided theranostics have also been widely developed. Recently, Dong and colleagues successfully designed a smart nanoplatform that could utilize the pH, hypoxia, and light as stimuli for imaging-guided combined therapy of cancer with minimized skin phototoxicity (Fig. 16) [217]. Harnessing the pH-responsive PS, ENAB, the melting point-tunable phase change material, and the hypoxia-activatable prodrug TPZ, the constructed NPs were able to self-adapt to sequential external and endogenous stimuli, ensuring efficient therapeutic specificity. Furthermore, a multifunctional platform enables the integration of multimode imaging guidance and synergistic integration of PTT, PDT, and chemotherapy to provide outstanding effectiveness. This work validated the necessity of combining imaging with various therapeutic strategies to combat dangerous tumors.

CONCLUSION AND OUTLOOK

With increasing expectations for the diagnosis and therapy of tumors, developing multifunctional nanosystems that integrate targeted drug delivery, *in vivo* tracing, effective therapy, and prognosis monitoring has received considerable attention. In this review, attention will be focused on the design ability of TME-specific strategies and nanotechnology, and we presented an exhaustive overview of different stimulus-responsive routes based on an acidic TME, enzyme overexpression, oxidation–reduction regulation, and hypoxic TME for the fabrication of nanostructures with various architectures, attractive characteristics, and versatile functions. These design strategies were highlighted, and their advantages and potential applications were discussed in detail, which may offer further guidance for ideas in designing novel functional nanomaterials.

Compared with other nanoarchitectures, TME-specific nanostructures exhibit prominent targeting capability and satisfactory therapeutic efficacy for cancer owing to their inherent EPR effects and multifunctional integration features. Although the relevant achievements are encouraging, many challenging issues still need to be resolved. First, the biological safety of the constructed nanomaterials needs to be urgently solved. It is necessary to develop materials with good biocompatibility and FDA-approved drugs for specific treatment of the TME to pave the way for clinical translational applications. Second, the therapeutic effect of nano-functional composites needs to be improved. Reasonable design and optimization of nanostructures is necessary, and the development of self-assembly strategies to arrange different functional molecules in an orderly manner is conducive to achieve the maximum drug loading and the ideal integration of multiple functions to improve the therapeutic effect of nanosystems. Finally, the relation between tumor diagnosis and treatment needs to be considered to develop more advanced biomaterials. Harnessing NIR-II imaging technology with deeper tissue penetration and less autofluorescence will further promote theranostic efficacy, realize the clear visualization of small tumor lesions and metastatic lesions, and enhance imaging-guided efficient tumor treatment. Future investigations may focus not only on many interesting nanosystems with more complicated architectures by combining diagnosis and treatment but also on understanding the mechanisms of functional nanomaterials for dealing with malignant diseases.

Acknowledgments: This work was supported by Hainan Provincial Natural Science Foundation of China (Nos. 819QN225 and 2019RC210), National Nature Science Foundation of China (Nos. 21961010, 21775162, 21864011, 21904030), Hainan Provincial Higher Education Research Project (Grants. Hnky2019ZD-29, Hnky2019ZD-30, Hnky2019ZD-52, Hnky2020-32), Talent Program of Hainan Medical University (Grants. HYPY201905, XRC180010, XRC180006, XRC180007, XRC190017, XRC190034, XRC190025), CAMS Innovation Fund for Medical Sciences (2019-I2M-5-023), Nanhai Young-Talent Program of Hainan (Grants. 20202018 and 20202007), and Hundred-Talent Program (Grants. Hainan 2018).

REFERENCES

1. Bray, F., Ferlay, J., Soerjomataram, I., Siegel, R.L., Torre, L.A. and Jemal, A., **2018**. Global cancer statistics 2018: GLOBOCAN estimates of incidence and mortality worldwide for 36 cancers in 185 countries. *CA—A Cancer Journal for Clinicians*, *68*(6), pp.394–424.
2. Brown, J.M. and Attardi, L.D., **2005**. Opinion—The role of apoptosis in cancer development and treatment response. *Nature Reviews Cancer*, *5*(3), pp.231–237.
3. Burrell, R.A., McGranahan, N., Bartek, J. and Swanton, C., **2013**. The causes and consequences of genetic heterogeneity in cancer evolution. *Nature*, *501*(7467), pp.338–345.
4. Paget, S., **1989**. The distribution of secondary growths in cancer of the breast. *Cancer Metastasis Reviews*, *8*(2), pp.98–101.
5. Joyce, J.A., **2005**. Therapeutic targeting of the tumor microenvironment. *Cancer Cell*, *7*(6), pp.513–520.
6. Galmarini, C.M. and Galmarini, F.C., **2003**. Multidrug resistance in cancer therapy: Role of the microenvironment. *Current Opinion in Investigational Drugs*, *4*(12), pp.1416–1421.
7. Fukumura, D. and Jain, R.K., **2007**. Tumor microenvironment abnormalities: Causes, consequences, and strategies to normalize. *Journal of Cellular Biochemistry*, *101*(4), pp.937–949.
8. Maier-Hauff, K., Ulrich, F., Nestler, D., Niehoff, H., Wust, P., Thiesen, B., Orawa, H., Budach, V. and Jordan, A., **2011**. Efficacy and safety of intratumoral thermotherapy using magnetic iron-oxide nanoparticles combined with external beam radiotherapy on patients with recurrent glioblastoma multiforme. *Journal of Neuro-Oncology*, *103*(2), pp.317–324.
9. Upreti, M., Jyoti, A. and Sethi, P., **2013**. Tumor microenvironment and nanotherapeutics. *Translational Cancer Research*, *2*(4), pp.309–319.
10. Nakasone, E.S., Askautrud, H.A., Kees, T., Park, J.H., Plaks, V., Ewald, A.J., Fein, M., Rasch, M. G., Tan, Y.X., Qiu, J., Park, J., Sinha, P., Bissell, M.J., Frengen, E., Werb, Z. and Egeblad, M., **2012**. Imaging tumor-stroma interactions during chemotherapy reveals contributions of the microenvironment to resistance. *Cancer Cell*, *21*(4), pp.488–503.
11. Kim, J. and Bae, J.S., **2016**. Tumor-associated macrophages and neutrophils in tumor microenvironment. *Mediators of Inflammation*, *2016*, pp.1–11.
12. Ji, T., Zhao, Y., Ding, Y. and Nie, G., **2013**. Using functional nanomaterials to target and regulate the tumor microenvironment: Diagnostic and therapeutic applications. *Advanced Materials*, *25*(26), pp.3508–3525.
13. Wong, X.Y., Sena-Torralba, A., Alvarez-Diduk, R., Muthoosamy, K. and Merkoci, A., **2020**. Nanomaterials for nanotheranostics: Tuning their properties according to disease needs. *ACS Nano*, *14*(3), pp.2585–2627.
14. Lammers, T., Aime, S., Hennink, W.E., Storm, G. and Kiessling, F., **2011**. Theranostic nanomedicine. *Accounts of Chemical Research*, *44*(10), pp.1029–1038.
15. Lin, Y., Zhuang, X., Xie, B. and Chen, H., **2020**. Enhanced antitumor efficacy of docetaxel-loaded monomethoxy poly(ethylene glycol)-poly(D,L-lactide-co-glycolide) amphiphilic copolymer against non-small cell lung cancer. *Journal of Nanoscience and Nanotechnology, 20*(12), pp.7263–7270.

16. Gao, M., Yu, F., Lv, C., Choo, J. and Chen, L., **2017**. Fluorescent chemical probes for accurate tumor diagnosis and targeting therapy. *Chemical Society Reviews*, *46*(8), pp.2237–2271.
17. Gao, M., Wang, R., Yu, F. and Chen, L., **2018**. Evaluation of sulfane sulfur bioeffects via a mitochondria-targeting selenium-containing near-infrared fluorescent probe. *Biomaterials*, *160*, pp.1–14.
18. Zou, Y., Li, M., Xing, Y., Duan, T., Zhou, X. and Yu, F., **2020**. Bioimaging of glutathione with a two-photon fluorescent probe and its potential application for surgery guide in laryngeal cancer. *ACS Sensors*, *5*(1), pp.242–249.
19. Ji, X., Yang, W., Wang, T., Mao, C., Guo, L., Xiao, J. and He, N., **2013**. Coaxially electrospun core/shell structured poly(Llactide) acid/chitosan nanofibers for potential drug carrier in tissue engineering. *Journal of Biomedical Nanotechnology, 9*(10), pp.1672–1678.
20. Peer, D., Karp, J.M., Hong, S., FaroKhzad, O.C., Margalit, R. and Langer, R., **2007**. Nanocarriers as an emerging platform for cancer therapy. *Nature Nanotechnology*, *2*(12), pp.751–760.
21. Jain, K.K., **2008**. Drug delivery systems-an overview. *Methods in Molecular Biology*, *437*, pp.1–50.
22. Shi, J., Votruba, A.R., Farokhzad, O.C. and Langer, R., **2010**. Nanotechnology in drug delivery and tissue engineering: From discovery to applications. *Nano Letters*, *10*(9), pp.3223–3230.
23. Zhang, L., Gu, F.X., Chan, J.M., Wang, A.Z., Langer, R.S. and Farokhzad, O.C., **2008**. Nanoparticles in medicine: Therapeutic applications and developments. *Clinical Pharmacology & Therapeutics*, *83*(5), pp.761–769.
24. Bottini, M., Sacchetti, C., Pietroiusti, A., Bellucci, S., Magrini, A., Rosato, N. and Bottini, N., **2014**. Targeted nanodrugs for cancer therapy: Prospects and challenges. *Journal of Nanoscience and Nanotechnology, 14*(1), 98–114.
25. Blanco, E., Shen, H. and Ferrari, M., **2015**. Principles of nanoparticle design for overcoming biological barriers to drug delivery. *Nature Biotechnology*, *33*(9), pp.941–951.
26. Rao, W., Wang, H., Zhong, A., Yu, J., Lu, X. and He, X., **2016**. Nanodrug-mediated thermotherapy of cancer stem-like cells. *Journal of Nanoscience and Nanotechnology, 16*(3), pp.2134–2142.
27. Song, X., Han, X., Yu, F., Zhang, X., Chen, L. and Lv, C., **2018**. Polyamine-targeting gefitinib prodrug and its near-infrared fluorescent theranostic derivative for monitoring drug delivery and lung cancer therapy. *Theranostics*, *8*(8), pp.2217–2228.
28. Zhang, X., He, N., Huang, Y., Yu, F., Li, B., Lv, C. and Chen, L., **2019**. Mitochondria-targeting near-infrared ratiometric fluorescent probe for selective imaging of cysteine in orthotopic lung cancer mice. *Sensors and Actuators B-Chemical*, *282*, pp.69–77.
29. Lin, G., Chen, S. and Mi, P., **2018**. Nanoparticles targeting and remodeling tumor microenvironment for cancer theranostics. *Journal of Biomedical Nanotechnology, 14*(7), pp.1189–1207.
30. Mo, R. and Gu, Z., **2016**. Tumor microenvironment and intracellular signal-activated nanomaterials for anticancer drug delivery. *Materials Today*, *19*(5), pp.274–283.
31. Gao, Z., Sun, J., Gao, M., Yu, F., Chen, L. and Chen, Q., **2018**. A unique off-on near-infrared cyanine-based probe for imaging of endogenous alkaline phosphatase activity in cells and in vivo. *Sensors and Actuators B-Chemical*, *265*, pp.565–574.
32. Wu, Z., Chen, J., Sun, Y., De Zhao, Shen, M., Huang, L. and Li, Y., **2018**. Tumor microenvironment-response calcium phosphate hybrid nanoparticles enhanced siRNAs targeting tumors in vivo. *Journal of Biomedical Nanotechnology, 14*(10), pp.1816–1825.
33. Maeda, H., Wu, J., Sawa, T., Matsumura, Y. and Hori, K., **2000**. Tumor vascular permeability and the EPR effect in macromolecular therapeutics: A review. *Journal of Controlled Release*, *65*(1–2), pp.271–284.
34. Liu, J., Ai, X., Zhang, H., Zhuo, W. and Mi, P., **2019**. Polymeric micelles with endosome escape and redox-responsive functions for enhanced intracellular drug delivery. *Journal of Biomedical Nanotechnology, 15*(2), pp.373–381.
35. Song, N., Lou, X.Y., Ma, L., Gao, H. and Yang, Y.W., **2019**. Supramolecular nanotheranostics based on pillarenes. *Theranostics*, *9*(11), pp.3075–3093.
36. Venkatraman, S.S., Ma, L.L., Natarajan, J.V. and Chattopadhyay, S., **2010**. Polymer- and liposome-based nanoparticles in targeted drug delivery. *Frontiers in Bioscience*, *2*, pp.801–814.
37. Yi, Y., Lin, G., Chen, S., Liu, J., Zhang, H. and Mi, P., **2018**. Polyester micelles for drug delivery and cancer theranostics: Current achievements, progresses and future perspectives. *Materials Science & Engineering C-Materials for Biological Applications*, *83*, pp.218–232.
38. Bhatnagar, S. and Venuganti, V.V.K., **2015**. Cancer targeting: Responsive polymers for stimuli-sensitive drug delivery. *Journal of Nanoscience and Nanotechnology, 15*(3), pp.1925–1945.
39. Lee, B.K., Yun, Y.H. and Park, K., **2015**. Smart nanoparticles for drug delivery: Boundaries and opportunities. *Chemical Engineering Science*, *125*, pp.158–164.
40. Li, J., Cheng, F., Huang, H., Li, L. and Zhu, J.J., **2015**. Nanomaterial-based activatable imaging probes: From design to biological applications. *Chemical Society Reviews*, *44*(21), pp.7855–7880.
41. Lee, S., Xie, J. and Chen, X., **2010**. Activatable molecular probes for cancer imaging. *Current Topics in Medicinal Chemistry*, *10*(11), pp.1135–1144.
42. Li, J., You, J., Dai, Y., Shi, M., Han, C. and Xu, K., **2014**. Gadolinium oxide nanoparticles and aptamer-functionalized silver nanoclusters-based multimodal molecular imaging nanoprobe for optical/magnetic resonance cancer cell imaging. *Analytical Chemistry*, *86*(22), pp.11306–11311.
43. Chen, Q., Wang, H., Liu, H., Wen, S., Peng, C., Shen, M., Zhang, G. and Shi, X., **2015**. Multifunctional dendrimer-entrapped gold nanoparticles modified with RGD peptide for targeted computed tomography/magnetic resonance dug-modal imaging of tumors. *Analytical Chemistry*, *87*(7), pp.3949–3956.
44. Long, S., Qiao, Q., Miao, L. and Xu, Z. **2019**. A self-assembly/disassembly two-photo ratiometric fluorogenic probe for bacteria imaging. *Chinese Chemical Letters*, *30*(3), pp.573–576.
45. Han, X., Song, X., Yu, F. and Chen, L., **2017**. A ratiometric fluorescent probe for imaging and quantifying anti-apoptotic effects of GSH under temperature stress. *Chemical Science*, *8*(10), pp.6991–7002.
46. Luo, X., Wang, R., Lv, C., Chen, G., You, J. and Yu, F., **2020**. Detection of selenocysteine with a ratiometric near-infrared fluorescent probe in cells and in mice thyroid diseases model. *Analytical Chemistry*, *92*(1), pp.1589–1597.
47. Garland, M., Yim, J.J. and Bogyo, M., **2016**. A bright future for precision medicine: Advances in fluorescent chemical probe design and their clinical application. *Cell Chemical Biology*, *23*(1), pp.122–136.
48. Wang, Y., Yu, F., Luo, X., Li, M., Zhao, L. and Yu, F., **2020**. Visualization of carboxylesterase 2 with a near-infrared two-photon fluorescent probe and potential evaluation of its anticancer drug effects in an orthotopic colon carcinoma mice model. *Chemical Communications*, *56*(32), pp.4412–4415.
49. Liu, H.W., Chen, L., Xu, C., Li, Z., Zhang, H., Zhang, X.B. and Tan, W., **2018**. Recent progresses in small-molecule enzymatic fluorescent probes for cancer imaging. *Chemical Society Reviews*, *47*(18), pp.7140–7180.
50. Kim, T., Huh, Y.M., Haam, S. and Lee, K., **2010**. Activatable nanomaterials at the forefront of biomedical sciences. *Journal of Materials Chemistry*, *20*(38), pp.8194–8206.
51. Kobayashi, H., Longmire, M.R., Ogawa, M. and Choyke, P.L., **2011**. Rational chemical design of the next generation of molecular imaging probes based on physics and biology: Mixing modalities, colors and signals. *Chemical Society Reviews*, *40*(9), pp.4626–4648.

52. Obliosca, J.M., Liu, C. and Yeh, H.C., **2013**. Fluorescent silver nanoclusters as DNA probes. *Nanoscale*, *5*(18), pp.8443–8461.

53. Drake, C.R., Miller, D.C. and Jones, E.F., **2011**. Activatable optical probes for the detection of enzymes. *Current Organic Synthesis*, *8*(4), pp.498–520.

54. Hou, J.T., Wang, B., Zou, Y., Fan, P., Chang, X., Cao, X., Wang, S. and Yu, F., **2020**. Molecular fluorescent probes for imaging and evaluation of hypochlorite fluctuations during diagnosis and therapy of osteoarthritis in cells and in a mouse model. *ACS Sensors*, *5*(7), pp.1949–1958.

55. Tang, C., Li, H., Hong, J. and Chai, X., **2020**. Application of nanoparticles in the early diagnosis and treatment of tumors: Current status and progress. *Traditional Medicine Research*, *5*(1), pp.34–43.

56. Zhu, C., Zhu, Y., Pan, H., Chen, Z. and Zhu, Q., **2019**. Current progresses of functional nanomaterials for imaging diagnosis and treatment of melanoma. *Current Topics in Medicinal Chemistry*, *19*(27), pp.2494–2506.

57. Hu, Y., Yu, C., Zhang, H., Wang, J., Jiang, G. and Kan, C., **2017**. pH-Triggered drug release of monodispersed P(St-co-DMAEMA) nanoparticles: Effects of swelling, polymer chain flexibility and drug-polymer interactions. *Journal of Nanoscience and Nanotechnology, 17*(2), pp.900–907.

58. Park, J., Choi, Y., Chang, H., Um, W., Ryu, J.H. and Kwon, I.C., **2019**. Alliance with EPR Effect: Combined strategies to improve the EPR effect in the tumor microenvironment. *Theranostics*, *9*(26), pp.8073–8090.

59. Bernier-Latmani, J. and Petrova, T.V., **2017**. Intestinal lymphatic vasculature: Structure, mechanisms and functions. *Nature Reviews Gastroenterology & Hepatology*, *14*(9), pp.510–526.

60. Matsumura, Y. and Maeda, H., **1986**. A new concept for macromolecular therapeutics in cancer chemotherapy: Mechanism of tumoritropic accumulation of proteins and the antitumor agent smancs. *Cancer Research*, *46*(12), pp.6387–6392.

61. Shi, J., Kantoff, P.W., Wooster, R. and Farokhzad, O.C., **2017**. Cancer nanomedicine: Progress, challenges and opportunities. *Nature Review Cancer*, *17*(1), pp.20–37.

62. Hartshorn, C.M., Bradbury, M.S., Lanza, G.M., Nel, A.E., Rao, J., Wang, A.Z., Wiesner, U.B., Yang, L. and Grodzinski, P., **2018**. Nanotechnology strategies to advance outcomes in clinical cancer care. *ACS Nano*, *12*(1), pp.24–43.

63. Nel, A., Ruoslahti, E. and Meng, H., **2017**. New insights into "permeability" as in the enhanced permeability and retention effect of cancer nanotherapeutics. *ACS Nano*, *11*(10), pp.9567–9569.

64. Fenaroli, F., Repnik, U., Xu, Y., Johann, K., Van Herck, S., Dey, P., Skjeldal, F.M., Frei, D.M., Bagherifam, S., Kocere, A., Haag, R., De Geest, B.G., Barz, M., Russell, D.G. and Griffiths, G., **2018**. Enhanced permeability and retention-like extravasation of nanoparticles from the vasculature into tuberculosis granulomas in zebrafish and mouse models. *ACS Nano*, *12*(8), pp.8646–8661.

65. Xia, Y., Tang, G., Wang, C., Zhong, J., Chen, Y., Hua, L., Li, Y., Liu, H., and Zhu, B., **2020**. Functionalized selenium nanoparticles for targeted siRNA delivery silence Derlin1 and promote antitumor efficacy against cervical cancer. *Drug Delivery*, *27*(1), pp.15–25.

66. Tang, L., Yang, X., Yin, Q., Cai, K., Wang, H., Chaudhury, I., Yao, C., Zhou, Q., Kwon, M., Hartman, J.A., Dobrucki, I.T., Dobrucki, L.W., Borst, L.B., Lezmi, S., Helferich, W.G., Ferguson, A.L., Fan, T.M. and Cheng, J., **2014**. Investigating the optimal size of anticancer nanomedicine. *Proceedings of the National Academy of Sciences of the United States of America*, *111*(43), pp.15344–15349.

67. Hobbs, S.K., Monsky, W.L., Yuan, F., Roberts, W.G., Griffith, L., Torchilin, V.P. and Jain, R.K., **1998**. Regulation of transport pathways in tumor vessels: Role of tumor type and microenvironment. *Proceedings of the National Academy of Sciences of the United States of America*, *95*(8), pp.4607–4612.

68. Ledda, M., Fioretti, D., Lolli, M.G., Papi, M., Di Gioia, C., Carletti, R., Ciasca, G., Foglia, S., Palmieri, V., Marchese, R., Grimaldi, S., Rinaldi, M., and Lisi, A., **2020**. Biocompatibility assessment of sub-5 nm silica-coated superparamagnetic iron oxide nanoparticles in human stem cells and in mice for potential application in nanomedicine. *Nanoscale*, *12*(3), pp.1759–1778.

69. Peng, C., Yu, M., Hsieh, J. T., Kapur, P. and Zheng, J., **2019**. Correlating anticancer drug delivery efficiency with vascular permeability of renal clearable versus non-renal clearable nanocarriers. *Angewandte Chemie International Edition*, *58*(35), pp.12076–12080.

70. Meng, H., Xue, M., Xia, T., Ji, Z., Tarn, D.Y., Zink, J.I. and Nel, A.E., **2011**. Use of size and a copolymer design feature to improve the biodistribution and the enhanced permeability and retention effect of doxorubicin-loaded mesoporous silica nanoparticles in a murine xenograft tumor model. *ACS Nano*, *5*(5), pp.4131–4144.

71. Sindhwani, S., Syed, A.M., Ngai, J., Kingston, B.R., Maiorino, L., Rothschild, J., MacMillan, P., Zhang, Y., Rajesh, N.U., Hoang, T., Wu, J.L.Y., Wilhelm, S., Zilman, A., Gadde, S., Sulaiman, A., Ouyang, B., Lin, Z., Wang, L., Egeblad, M. and Chan, W.C.W., **2020**. The entry of nanoparticles into solid tumours. *Nature Materials*, *19*(5), pp.566–575.

72. Jin, Q., Deng, Y., Chen, X. and Ji, J., **2019**. Rational design of cancer nanomedicine for simultaneous stealth surface and enhanced cellular uptake. *ACS Nano*, *13*(2), pp.954–977.

73. Gulzar, A., Xu, J., Wang, C., He, F., Yang, D., Gai, S., Yang, P., Lin, J., Jin, D. and Xing, B., **2019**. Tumour microenvironment responsive nanoconstructs for cancer theranostic. *Nano Today*, *26*, pp.16–56.

74. Wilhelm, S., Tavares, A.J., Dai, Q., Ohta, S., Audet, J., Dvorak, H.F. and Chan, W.C., **2016**. Analysis of nanoparticle delivery to tumours. *Nature Reviews Materials*, *1*(5), pp.1–12.

75. Ekladious, I., Colson, Y.L. and Grinstaff, M.W., **2019**. Polymer-drug conjugate therapeutics: Advances, insights and prospects. *Nature Reviews Drug Discovery*, *18*(4), pp.273–294.

76. Chen, E., Chen, B.M., Su, Y.C., Chang, Y.C., Cheng, T.L., Barenholz, Y. and Roffler, S.R., **2020**. Premature drug release from polyethylene glycol (PEG)-coated liposomal doxorubicin via formation of the membrane attack complex. *ACS Nano*, *14*(7), pp.7808–7822.

77. Jain, S., Dongave, S.M., Date, T., Kushwah, V., Mahajan, R.R., Pujara, N., Kumeria, T. and Popat, A., **2019**. Succinylated β-Lactoglobuline-functionalized multiwalled carbon nanotubes with improved colloidal stability and biocompatibility. *ACS Biomaterials Science & Engineering*, *5*(7), pp.3361–3372.

78. Dai, Y., Xu, C., Sun, X. and Chen, X., **2017**. Nanoparticle design strategies for enhanced anticancer therapy by exploiting the tumour microenvironment. *Chemical Society Reviews*, *46*(12), pp.3830–3852.

79. Tian, W., Lu, J. and Jiao, D., **2019**. Stem cell membrane vesicle-coated nanoparticles for efficient tumor-targeted therapy of orthotopic breast cancer. *Polymers for Advanced Technologies*, *30*(4), pp.1051–1060.

80. Uthaman, S., Huh, K.M. and Park, I.K., **2018**. Tumor microenvironment-responsive nanoparticles for cancer theragnostic applications. *Biomaterials Research*, *22*, pp.1–11.

81. Bazak, R., Houri, M., El Achy, S., Kamel, S. and Refaat, T., **2015**. Cancer active targeting by nanoparticles: A comprehensive review of literature. *Journal of Cancer Research and Clinical Oncology*, *141*(5), pp.769–784.

82. Youn, Y.S. and Bae, Y.H., **2018**. Perspectives on the past, present, and future of cancer nanomedicine. *Advanced Drug Delivery Reviews*, *130*, pp.3–11.

83. Wang, S., Huang, P. and Chen, X., **2016**. Stimuli-responsive programmed specific targeting in nanomedicine. *ACS Nano*, *10*(3), pp.2991–2994.

84. Tsvetkova, Y., Beztsinna, N., Baues, M., Klein, D., Rix, A., Golombek, S.K., Al Rawashdeh, W., Gremse, F., Barz, M.,

Koynov, K., Banala, S., Lederle, W., Lammers, T. and Kiessling, F., **2017**. Balancing passive and active targeting to different tumor compartments using riboflavin-functionalized polymeric nanocarriers. *Nano Letters*, *17*(8), pp.4665–4674.

85. Apte, R.S., Chen, D.S. and Ferrara, N., **2019**. VEGF in signaling and disease: Beyond discovery and development. *Cell*, *176*(6), pp.1248–1264.

86. Goel, S., Chen, F., Hong, H., Valdovinos, H.F., Hernandez, R., Shi, S., Barnhart, T.E. and Cai, W., **2014**. VEGF121-conjugated mesoporous silica nanoparticle: A tumor targeted drug delivery system. *ACS Applied Materials & Interfaces*, *6*(23), pp.21677–21685.

87. Arosio, D. and Casagrande, C., **2016**. Advancement in integrin facilitated drug delivery. *Advanced Drug Delivery Reviews*, *97*, pp.111–143.

88. Duro-Castano, A., Gallon, E., Decker, C. and Vicent, M.J., **2017**. Modulating angiogenesis with integrin-targeted nanomedicines. *Advanced Drug Delivery Reviews*, *119*, pp.101–119.

89. Zhu, P., Gao, S., Lin, H., Lu, X., Yang, B., Zhang, L., Chen, Y. and Shi, J., **2019**. Inorganic nanoshell-stabilized liquid metal for targeted photonanomedicine in NIR-II biowindow. *Nano Letters*, *19*(3), pp.2128–2137.

90. Chen, X. and Song, E., **2019**. Turning foes to friends: Targeting cancer-associated fibroblasts. *Nature Reviews Drug Discovery*, *18*(2), pp.99–115.

91. Tan, T., Hu, H., Wang, H., Li, J., Wang, Z., Wang, J., Wang, S., Zhang, Z. and Li, Y., **2019**. Bioinspired lipoproteins-mediated photothermia remodels tumor stroma to improve cancer cell accessibility of second nanoparticles. *Nature Communications*, *10*(1), p.3322.

92. Miao, L., Liu, Q., Lin, C.M., Luo, C., Wang, Y., Liu, L., Yin, W., Hu, S., Kim, W.Y. and Huang, L., **2017**. Targeting tumor-associated fibroblasts for therapeutic delivery in desmoplastic tumors. *Cancer Research*, *77*(3), pp.719–731.

93. Ernsting, M.J., Hoang, B., Lohse, I., Undzys, E., Cao, P., Do, T., Gill, B., Pintilie, M., Hedley, D. and Li, S.D., **2015**. Targeting of metastasis-promoting tumor-associated fibroblasts and modulation of pancreatic tumor-associated stroma with a carboxymethylcellulose-docetaxel nanoparticle. *Journal of Controlled Release*, *206*, pp.122–130.

94. Lambert, A.W., Pattabiraman, D.R. and Weinberg, R.A., **2017**. Emerging biological principles of metastasis. *Cell*, *168*(4), pp.670–691.

95. Schroeder, A., Heller, D.A., Winslow, M.M., Dahlman, J.E., Pratt, G.W., Langer, R., Jacks, T. and Anderson, D.G., **2011**. Treating metastatic cancer with nanotechnology. *Nature Reviews Cancer*, *12*(1), pp.39–50.

96. Akinc, A., Zumbuehl, A., Goldberg, M., Leshchiner, E.S., Busini, V., Hossain, N., Bacallado, S. A., Nguyen, D.N., Fuller, J., Alvarez, R., Borodovsky, A., Borland, T., Constien, R., de Fougerolles, A., Dorkin, J.R., Narayanannair Jayaprakash, K., Jayaraman, M., John, M., Koteliansky, V., Manoharan, M., Nechev, L., Qin, J., Racie, T., Raitcheva, D., Rajeev, K.G., Sah, D.W., Soutschek, J., Toudjarska, I., Vornlocher, H.P., Zimmermann, T.S., Langer, R. and Anderson, D.G., **2008**. A combinatorial library of lipid-like materials for delivery of RNAi therapeutics. *Nature Biotechnology*, *26*(5), pp.561–569.

97. Rychahou, P., Haque, F., Shu, Y., Zaytseva, Y., Weiss, H. L., Lee, E.Y., Mustain, W., Valentino, J., Guo, P. and Evers, B.M., **2015**. Delivery of RNA nanoparticles into colorectal cancer metastases following systemic administration. *ACS Nano*, *9*(2), pp.1108–1116.

98. Feng, L., Dong, Z., Tao, D., Zhang, Y. and Liu, Z., **2018**. The acidic tumor microenvironment: A target for smart cancer nanotheranostics. *National Science Review*, *5*(2), pp.269–286.

99. Wang, M., Chen, M., Niu, W., Winston, W., Cheng, W., ang Lei, B., **2020**. Injectable biodegradation-visual self-healing citrate hydrogel with high tissue penetration for microenvironment-responsive degradation and local tumor therapy. *Biomaterials, 261*, pp.1–12.

100. Wu, Y., Zhang, W., Li, J. and Zhang, Y., **2013**. Optical imaging of tumor microenvironment. *American Journal of Nuclear Medicine and Molecular Imaging*, *3*(1), pp.1–15.

101. Zhou, Z. and Lu, Z.R., **2017**. Molecular imaging of the tumor microenvironment. *Advanced Drug Delivery Reviews, 113*, pp.24–48.

102. Li, J., Cheng, F., Huang, H., Li, L. and Zhu, J.J., **2015**. Nanomaterial-based activatable imaging probes: From design to biological applications. *Chemical Society Reviews*, *44*(21), pp.7855–7880.

103. Huang, X., Song, J., Yung, B. C., Huang, X., Xiong, Y. and Chen, X., **2018**. Ratiometric optical nanoprobes enable accurate molecular detection and imaging. *Chemical Society Reviews*, *47*(8), pp.2873–2920.

104. Lei, Y., He, X., Tang, J., Shi, H., He, D., Yan, L., Liu, J., Zeng, Y. and Wang, K., **2018**. Ultra-pH-responsive split i-motif based aptamer anchoring strategy for specific activatable imaging of acidic tumor microenvironment. *Chemical Communications*, *54*(73), pp.10288–10291.

105. Shi, H., Lei, Y., Ge, J., He, X., Cui, W., Ye, X., Liu, J. and Wang, K., **2019**. A Simple, pH-activatable fluorescent aptamer probe with ultralow background for bispecific tumor imaging. *Analytical Chemistry*, *91*(14), pp.9154–9160.

106. Dai, C., Lin, H., Xu, G., Liu, Z., Wu, R., and Chen, Y., **2017**. Biocompatible 2D titanium carbide (MXenes) composite nanosheets for pH-responsive MRI-guided tumor hyperthermia. *Chemistry of Materials*, *29*(20), pp.8637–8652.

107. Liu, Y., Bhattarai, P., Dai, Z. and Chen, X., **2019**. Photothermal therapy and photoacoustic imaging via nanotheranostics in fighting cancer. *Chemical Society Reviews*, *48*(7), pp.2053–2108.

108. Song, X., Chen, Q. and Liu, Z., **2014**. Recent advances in the development of organic photothermal nano-agents. *Nano Research*, *8*(2), pp.340–354.

109. Xue, F., Wen, Y., Wei, P., Gao, Y., Zhou, Z., Xiao, S. and Yi, T., **2017**. A smart drug: A pH-responsive photothermal ablation agent for Golgi apparatus activated cancer therapy. *Chemical Communications*, *53*(48), pp.6424–6427.

110. Guo, M., Huang, J., Deng, Y., Shen, H., Ma, Y., Zhang, M., Zhu, A., Li, Y., Hui, H., Wang, Y., Yang, X., Zhang, Z. and Chen, H., **2015**. pH-Responsive cyaninegrafted graphene oxide for fluorescence resonance energy transfer-enhanced photothermal therapy. *Advanced Functional Materials*, *25*(1), pp.59–67.

111. Gao, G., Jiang, Y. W., Sun, W., Guo, Y., Jia, H.R., Yu, X.W., Pan, G.Y. and Wu, F.G., **2019**. Molecular targeting-mediated mild-temperature photothermal therapy with a smart albumin-based nanodrug. *Small*, *15*(33), pp.1–15.

112. Lan, M., Zhao, S., Liu, W., Lee, C. S., Zhang, W. and Wang, P., **2019**. Photosensitizers for photodynamic therapy. *Advanced Healthcare Materials*, *8*(13), pp.1–37.

113. Li, L., Chen, Y., Chen, Q., Tan, Y., Chen, H. and Yin, J., **2019**. Photodynamic therapy based on organic small molecular fluorescent dyes. *Chinese Chemical Letters, 30*(10), pp.1689–1703.

114. Shen, L., Huang, Y., Chen, D., Qiu, F., Ma, C., Jin, X., Zhu, X., Zhou, G. and Zhang, Z., **2017**. pH-responsive aerobic nanoparticles for effective photodynamic therapy. *Theranostics*, *7*(18), pp.4537–4550.

115. Yang, Z., Chen, Q., Chen, J., Dong, Z., Zhang, R., Liu, J. and Liu, Z., **2018**. Tumor-pH-responsive dissociable albumin-tamoxifen nanocomplexes enabling efficient tumor penetration and hypoxia relief for enhanced cancer photodynamic therapy. *Small*, *14*(49), pp.1–10.

116. Li, F., Du, Y., Liu, J., Sun, H., Wang, J., Li, R., Kim, D., Hyeon, T. and Ling, D., **2018**. Responsive assembly of upconversion nanoparticles for pH-activated and near-infrared-triggered photodynamic therapy of deep tumors. *Advanced Materials*, *30*(35), pp.1–7.

117. Nomoto, T., Fukushima, S., Kumagai, M., Miyazaki, K., Inoue, A., Mi, P., Maeda, Y., Toh, K., Matsumoto, Y., Morimoto, Y.,

Kishimura, A., Nishiyama, N. and Kataoka, K., **2016**. Calcium phosphate-based organic–inorganic hybrid nanocarriers with pH-responsive on/off switch for photodynamic therapy. *Biomaterials Science*, *4*(5), pp.826–838.

118. Qi, T., Chen, B., Wang, Z., Du, H., Liu, D., Yin, Q., Liu, B., Zhang, Q. and Wang, Y., **2019**. A pH-Activatable nanoparticle for dual-stage precisely mitochondria-targeted photodynamic anticancer therapy. *Biomaterials*, *213*, pp.1–12.

119. Yan, C., Shi, L., Guo, Z. and Zhu, W., **2019**. Molecularly near-infrared fluorescent theranostics for in vivo tracking tumor-specific chemotherapy. *Chinese Chemical Letters, 30*(10), pp.1849–1855.

120. Dai, L., Li, X., Duan, X., Li, M., Niu, P., Xu, H., Cai, K., and Yang, H., **2019**. A pH/ROS cascade-responsive charge-reversal nanosystem with self-amplified drug release for synergistic oxidation-chemotherapy. *Advanced Science*, *6*(4), pp.1–13.

121. Li, Z., Wang, H., Chen, Y., Wang, Y., Li, H., Han, H., Chen, T., Jin, Q. and Ji, J., **2016**. pH- and NIR light-responsive polymeric prodrug micelles for hyperthermia-assisted site-specific chemotherapy to reverse drug resistance in cancer treatment. *Small*, *12*(20), pp.2731–2740.

122. Cai, X., Luo, Y., Yan, H., Du, D. and Lin, Y., **2017**. pH-Responsive ZnO nanocluster for lung cancer chemotherapy. *ACS Applied Materials & Interfaces*, *9*(7), pp.5739–5747.

123. Galluzzi, L., Chan, T.A., Kroemer, G., Wolchok, J.D. and Lopez-Soto, A., **2018**. The hallmarks of successful anticancer immunotherapy. *Science Translational Medicine*, *10*(459), pp.1–15.

124. Yang, Z., Ma, Y., Zhao, H., Yuan, Y. and Kim, B.Y.S., **2020**. Nanotechnology platforms for cancer immunotherapy. *Wiley Interdisciplinary Reviews Nanomedicine and Nanobiotechnology*, *12*(2), pp.1–28.

125. Riley, R.S., June, C.H., Langer, R. and Mitchell, M.J., **2019**. Delivery technologies for cancer immunotherapy. *Nature Reviews Drug Discovery*, *18*(3), pp.175–196.

126. Duan, F., Feng, X., Yang, X., Sun, W., Jin, Y., Liu, H., Ge, K., Li, Z. and Zhang, J., **2017**. A simple and powerful co-delivery system based on pH-responsive metal-organic frameworks for enhanced cancer immunotherapy. *Biomaterials*, *122*, pp.23–33.

127. Kim, H., Sehgal, D., Kucaba, T.A., Ferguson, D.M., Griffith, T.S. and Panyam, J., **2018**. Acidic pH-responsive polymer nanoparticles as a TLR7/8 agonist delivery platform for cancer immunotherapy. *Nanoscale*, *10*(44), pp.20851–20862.

128. Zhang, Z., Wang, Q., Liu, Q., Zheng, Y., Zheng, C., Yi, K., Zhao, Y., Gu, Y., Wang, Y., Wang, C., Zhao, X., Shi, L., Kang, C. and Liu, Y., **2019**. Dual-locking nanoparticles disrupt the PD-1/PD-L1 pathway for efficient cancer immunotherapy. *Advanced Materials*, *31*(51), pp.1–10.

129. Wang, Y., Huang, X., Tang, Y., Zou, J., Wang, P., Zhang, Y., Si, W., Huang, W. and Dong, X., **2018**. A light-induced nitric oxide controllable release nano-platform based on diketopyrrolopyrrole derivatives for pH-responsive photodynamic/photothermal synergistic cancer therapy. *Chemical Science*, *9*(42), pp.8103–8109.

130. Jiang, B.P., Zhang, L., Guo, X.L., Shen, X.C., Wang, Y., Zhu, Y., and Liang, H., **2017**. Poly(N-phenylglycine)-based nanoparticles as highly effective and targeted near-infrared photothermal therapy/photodynamic therapeutic agents for malignant melanoma. *Small*, *13*(8), pp.1–15.

131. Li, Y., Lin, J., Wang, P., Luo, Q., Lin, H., Zhang, Y., Hou, Z., Liu, J. and Liu, X., **2019**. Tumor microenvironment responsive shape-reversal self-targeting virus-inspired nanodrug for imaging-guided near-infrared-II photothermal chemotherapy. *ACS Nano*, *13*(11), pp.12912–12928.

132. Yang, W., Zhang, F., Deng, H., Lin, L., Wang, S., Kang, F., Yu, G., Lau, J., Tian, R., Zhang, M., Wang, Z., He, L., Ma, Y., Niu, G., Hu, S. and Chen, X., **2020**. Smart nanovesicle-mediated immunogenic cell death through tumor microenvironment modulation for effective photodynamic immunotherapy. *ACS Nano*, *14*(1), pp.620–631.

133. Egeblad, M. and Werb, Z., **2002**. New functions for the matrix metalloproteinases in cancer progression. *Nature Reviews Cancer*, *2*(3), pp.161–174.

134. Ahmad, R., Deng, Y., Singh, R., Hussain, M., Shah, M.A.A., Elingarami, S., He, N. and Sun, Y., **2018**. Cutting edge protein and carbohydrate-based materials for anticancer drug delivery. *Journal of Biomedical Nanotechnology*, *14*(1), pp.20–43.

135. Li, L., Fu, S., Chen, C., Wang, X., Fu, C., Wang, S., Guo, W., Yu, X., Zhang, X., Liu, Z., Qiu, J.M. and Liu, H., **2016**. Microenvironment-driven bioelimination of magnetoplasmonic nanoassemblies and their multimodal imaging-guided tumor photothermal therapy. *ACS Nano*, *10*(7), pp.7094–7105.

136. Sun, Z., Cheng, K., Yao, Y., Wu, F., Fung, J., Chen, H., Ma, X., Tu, Y., Xing, L., Xia, L. and Cheng, Z., **2019**. Controlled nano-biointerface of functional nanoprobes for in vivo monitoring enzyme activity in tumors. *ACS Nano*, *13*(2), pp.1153–1167.

137. Cheng, D.B., Wang, D., Gao, Y.J., Wang, L., Qiao, Z.Y. and Wang, H., **2019**. Autocatalytic morphology transformation platform for targeted drug accumulation. *Journal of the American Chemical Society*, *141*(10), pp.4406–4411.

138. Li, N., Li, N., Yi, Q., Luo, K., Guo, C., Pan, D. and Gu, Z., **2014**. Amphiphilic peptide dendritic copolymer-doxorubicin nanoscale conjugate self-assembled to enzyme-responsive anti-cancer agent. *Biomaterials*, *35*(35), pp.9529–9545.

139. Jiang, T., Mo, R., Bellotti, A., Zhou, J. and Gu, Z., **2014**. Gel-liposome-mediated co-delivery of anticancer membrane-associated proteins and small-molecule drugs for enhanced therapeutic efficacy. *Advanced Functional Materials*, *24*(16), pp.2295–2304.

140. Yuan, Y., Ding, Z., Qian, J., Zhang, J., Xu, J., Dong, X., Han, T., Ge, S., Luo, Y., Wang, Y., Zhong, K. and Liang, G., **2016**. Casp3/7-iInstructed intracellular aggregation of Fe_3O_4 nanoparticles enhances T-2 MR imaging of tumor apoptosis. *Nano Letters*, *16*(4), pp.2686–2691.

141. Zhou, R., Zhu, S., Gong, L., Fu, Y., Gu, Z. and Zhao, Y., **2019**. Recent advances of stimuli-responsive systems based on transition metal dichalcogenides for smart cancer therapy. *Journal of Materials Chemistry B*, *7*(16), pp.2588–2607.

142. Chen, D., Qin, W., Fang, H., Wang, L., Peng, B., Li, L. and Huang, W., **2019**. Molecularly near-infrared fluorescent theranostics for in vivo tracking tumor-specific chemotherapy. *Chinese Chemical Letters, 30*(10), pp.1738–1744.

143. Gao, X., Li, J., Luan, M., Li, Y., Pan, W., Li, N. and Tang, B., **2020**. Real-time in situ monitoring of signal molecules' evolution in apoptotic pathway via Au–Se bond constructed nanoprobe. *Biosensors and Bioelectronics*, *147*, pp.1–8.

144. Luan, M., Li, N., Pan, W., Yang, L., Yu, Z. and Tang, B., **2017**. Simultaneous detection of multiple targets involved in the PI3K/AKT pathway for investigating cellular migration and invasion with a multicolor fluorescent nanoprobe. *Chemical Communications*, *53*(2), pp.356–359.

145. Hou, Y., Zhou, J., Gao, Z., Sun, X., Liu, C., Shangguan, D., Yang, W., and Gao, M., **2015**. Protease-activated ratiometric fluorescent probe for pH mapping of malignant tumors. *ACS Nano*, *9*(3), pp.3199–3205.

146. Ma, T., Hou, Y., Zeng, J., Liu, C., Zhang, P., Jing, L., Shangguan, D. and Gao, M., **2018**. Dual-ratiometric target-triggered fluorescent probe for simultaneous quantitative visualization of tumor microenvironment protease activity and pH in vivo. *Journal of the American Chemical Society*, *140*(1), pp.211–218.

147. Nguyen, P.D., Cong, V.T., Baek, C. and Min, J., **2017**. Fabrication of peptide stabilized fluorescent gold nanocluster/graphene oxide nanocomplex and its application in turn-on detection of metalloproteinase-9. *Biosensors and Bioelectronics*, *89*, pp.666–672.

148. Zhang, X., Miao, Z., Hu, Y., Yang, X., Tang, Y. and Zhu, D., **2018**. Programmed microcapsule-type matrix metalloproteinase-2

(MMP-2)-responsive nanosensor for in situ monitoring of intracellular MMP-2. *Sensors and Actuators B: Chemical*, *273*, pp.511–518.

149. Huang, Y., Shi, M., Hu, K., Zhao, S., Lu, X., Chen, Z.F., Chen, J. and Liang, H., **2013**. Carbon nanotube-based multicolor fluorescent peptide probes for highly sensitive multiplex detection of cancer-related proteases. *Journal of Materials Chemistry B*, *1*(28), pp.3470–3476.

150. Yang, J.K., Hwang, I.J., Jeon, S.J., Ju, J.M., Kim, H.I., Yim, D., Lee, Y.S. and Kim, J.H., **2019**. Atomically-tailored graphene oxide displaying enhanced fluorescence for the improved optical sensing of MMP-2, *Sensors and Actuators B: Chemical*, *284*, pp.485–493.

151. Langer, J., Jimenez de Aberasturi, D., Aizpurua, J., Alvarez-Puebla, R.A., Auguié, B., Baumberg, J.J., Bazan, G.C., Bell, S.E.J., Boisen, A. and Brolo, A.G., **2020**. Present and future of surface-enhanced Raman scattering. *ACS Nano*, *14*(1), pp.28–117.

152. Gong, T., Kong, K.V., Goh, D., Olivo, M. and Yong, K.T., **2015**. Sensitive surface enhanced Raman scattering multiplexed detection of matrix metalloproteinase 2 and 7 cancer markers. *Biomedical Optics Express*, *6*(6), pp.2076–2087.

153. Gong, T., Hong, Z.Y., Chen, C.H., Tsai, C.Y., Liao, L.D. and Kong, K.V., **2017**. Optical interference-free surface-enhanced raman scattering CO-nanotags for logical multiplex detection of vascular disease-related biomarkers. *ACS Nano*, *11*(3), pp.3365–3375.

154. Lin, D., Tseng, C.Y., Lim, Q.F., Tan, M.J. and Kong, K.V., **2018**. A rapid and highly sensitive strain-effect graphene-based bio-sensor for the detection of stroke and cancer bio-markers. *Journal of Materials Chemistry B*, *6*(17), pp.2536–2540.

155. Zhao, L., Xing, Y., Wang, R., Yu, F. and Yu, F., **2020**. Self-qssembled nanomaterials for enhanced phototherapy of cancer. *ACS Applied Bio Materials*, *3*(1), pp.86–106.

156. Gandhi, S., Arami, H. and Krishnan, K.M., **2016**. Detection of cancer-specific proteases using magneticrelaxation of peptide-conjugated nanoparticles in biological environment. *Nano Letters*, *16*(6), pp.3668–3674.

157. Zhu, X., Lin, H., Wang, L., Tang, X., Ma, L., Chen, Z. and Gao, J., **2017**. Activatable T1 relaxivity recovery nanoconjugates for kinetic and sensitive analysis of matrix metalloprotease 2. *ACS Applied Materials & Interfaces*, *9*(26), pp.21688–21696.

158. Schuerle, S., Dudani, J.S., Christiansen, M.G., Anikeeva, P. and Bhatia, S.N., **2016**. Magnetically actuated protease sensors for in vivo tumor profiling. *Nano Letters*, *16*(10), pp.6303–6310.

159. Yang, K., Zhu, L., Nie, L., Sun, X., Cheng, L., Wu, C., Niu, G., Chen, X. and Liu, Z., **2014**. Visualization of protease activity in vivo using an activatable photo-acoustic imaging probe cased on CuS nanoparticles. *Theranostics*, *4*(2), pp.134–141.

160. Zhang, D., Qi, G.B., Zhao, Y.X., Qiao, S.L., Yang, C. and Wang, H., **2015**. In situ formation of nanofibers from purpurin18-peptide conjugates and the assembly induced retention effect in tumor sites. *Advanced Materials*, *27*(40), pp.6125–6130.

161. Yin, L., Sun, H., Zhang, H., He, L., Qiu, L., Lin, J., Xia, H., Zhang, Y., Ji, S., Shi, H. and Gao, M., **2019**. Quantitatively visualizing tumor-related protease activity in vivo using a ratiometric photoacoustic probe. *Journal of the American Chemical Society*, *141*(7), pp.3265–3273.

162. Yuan, Y., Wang, L., Du, W., Ding, Z., Zhang, J., Han, T., An, L., Zhang, H. and Liang, G., **2015**. Intracellular self-assembly of taxol nanoparticles for overcoming multidrug resistance. *Angewandte Chemie International Edition*, *54*(33), pp.9700–9704.

163. Tao, F., Han, Q., Liu, K. and Yang, P., **2017**. Tuning crystallization pathways through the mesoscale assembly of biomacromolecular nanocrystals. *Angewandte Chemie International Edition*, *56*(43), pp.13440–13444.

164. Kalafatovic, D., Nobis, M., Son, J., Anderson, K. and Ulijn, R.V., **2016**. MMP-9 triggered self-assembly of doxorubicin nanofiber depots halts tumor growth. *Biomaterials*, *98*, pp.192–202.

165. Ai, X., Ho, C.J.H., Aw, J., Attia, A.B.E., Mu, J., Wang, Y., Wang, X., Wang, Y., Liu, X., Chen, H., Gao, M., Chen, X., Yeow, E.K.L., Liu, G., Olivo, M. and Xing, B., **2016**. In vivo covalent cross-linking of photon-converted rare-earth nanostructures for tumour localization and theranostics. *Nature Communications*, *7*, pp.1–9.

166. Li, M., Gao, Y., Yuan, Y., Wu, Y., Song, Z., Tang, B.Z., Liu, B. and Zheng, Q.C., **2017**. One-step formulation of targeted aggregation-induced emission dots for image-guided photodynamic therapy of cholangiocarcinoma. *ACS Nano*, *11*(4), pp.3922–3932.

167. Hu, B., Li, P., Zhang, Y., Shan, C., Su, P., Cao, J., Cheng, B., Wu, W., Liu, W. and Tang, Y., **2019**. Activatable smart nanoprobe for sensitive endogenous MMP2 detection and fluorescence imaging-guided phototherapies. *Inorganic Chemistry Frontiers*, *6*(3), pp.820–828.

168. Zhao, X., Yang, C.X., Chen, L.G. and Yan, X.P., **2017**. Dual-stimuli responsive and reversibly activatable theranostic nanoprobe for precision tumor-targeting and fluorescence-guided photothermal therapy. *Nature Communications*, *8*(1), pp.1–9.

169. Wang, J., Liu, J., Liu, Y., Wang, L., Cao, M., Ji, Y., Wu, X., Xu, Y., Bai, B., Miao, Q., Chen, C. and Zhao, Y., **2016**. Gd-Hybridized plasmonic Au-nanocomposites enhanced tumor-interior drug permeability in multimodal imaging-guided therapy. *Advanced Materials*, *28*(40), pp.8950–8958.

170. Dong, X., Yin, W., Zhang, X., Zhu, S., He, X., Yu, J., Xie, J., Guo, Z., Yan, L., Liu, X., Wang, Q., Gu, Z. and Zhao, Y., **2018**. Intelligent MoS_2 nanotheranostic for targeted and enzyme-/pH-/NIR-Responsive drug delivery to overcome cancer chemotherapy resistance guided by PET imaging. *ACS Applied Materials & Interfaces*, *10*(4), pp.4271–4284.

171. Halliwell, B., **1991**. Reactive oxygen species in living systems: Source, biochemistry, and role in human disease. *The American Journal of Medicine*, *91*(3), pp.S14–S22.

172. Pastore, A., Federici, G., Bertini, E. and Piemonte, F., **2003**. Analysis of glutathione: Implication in redox and detoxification. *Clinica Chimica Acta*, *333*(1), pp.19–39.

173. Najafi, M., Goradel, N.H., Farhood, B., Salehi, E., Solhjoo, S., Toolee, H., Kharazinejad, E. and Mortezaee, K., **2019**. Tumor microenvironment: Interactions and therapy. *Journal of Cellular Physiology*, *234*(5), pp.5700–5721.

174. Qin, X. and Li, Y., **2020**. Strategies to design and synthesize polymer-based stimuli-responsive drug-delivery nanosystems. *ChemBioChem*, *21*(9), pp.1236–1253.

175. Gong, F., Yang, N., Wang, X., Zhao, Q., Chen, Q., Liu, Z. and Cheng, L., **2020**. Tumor microenvironment-responsive intelligent nanoplatforms for cancer theranostics. *Nano Today*, *32*, pp.1–28.

176. Ye, H., Zhou, Y., Liu, X., Chen, Y., Duan, S., Zhu, R., Liu, Y. and Yin, L., **2019**. Recent advances on reactive oxygen species-responsive felivery and diagnosis system. *Biomacromolecules*, *20*(7), pp.2441–2463.

177. Yan, K.C., Sedgwick, A.C., Zang, Y., Chen, G.R., He, X.P., Li, J., Yoon, J. and James, T.D., **2019**. Sensors, imaging agents, and theranostics to help understand and treat reactive oxygen species related diseases. *Small Methods*, *3*(7), pp.1–42.

178. Saravanakumar, G., Kim, J. and Kim, W.J., **2017**. Reactive-oxygen-species-responsive drug delivery systems: promises and challenges. *Advanced Science*, *4*(1), pp.1–19.

179. Szatrowski, T.P. and Nathan, C.F., **1991**. Production of large amounts of hydrogen peroxide by human tumor cells. *Cancer Research*, *51*(3), pp.794–798.

180. Yang, N., Xiao, W., Song, X., Wang, W. and Dong, X., **2020**. Recent advances in tumor microenvironment hydrogen peroxide-responsive materials for cancer photodynamic therapy. *Nano-Micro Letters*, *12*(1), pp.1–27.

181. Stubelius, A., Lee, S. and Almutairi, A., **2019**. The chemistry of boronic acids in nanomaterials for drug delivery. *Accounts of Chemical Research*, *52*(11), pp.3108–3119.

182. Wang, J., Zhang, Y., Archibong, E., Ligler, F.S. and Gu, Z., **2017**. Leveraging H_2O_2 levels for biomedical applications. *Advanced Biosystems*, *1*(9), pp.1–15.

183. Luo, C.Q., Xing, L., Cui, P.F., Qiao, J.B., He, Y.J., Chen, B.A., Jin, L. and Jiang, H.L., **2017**. Curcumin-coordinated nanoparticles with improved stability for reactive oxygen species-responsive drug delivery in lung cancer therapy. *International Journal of Nanomedicine*, *12*, pp.855–869.

184. Zhang, M., Song, C.C., Su, S., Du, F.S. and Li, Z.C., **2018**. ROS-zctivated ratiometric fluorescent polymeric nanoparticles for self-reporting drug delivery. *ACS Applied Materials & Interfaces*, *10*(9), pp.7798–7810.

185. Dong, C., Zhou, Q., Xiang, J., Liu, F., Zhou, Z. and Shen, Y., **2020**. Self-assembly of oxidation-responsive polyethylene glycol-paclitaxel prodrug for cancer chemotherapy. *Journal of Controlled Release*, *321*, pp.529–539.

186. Liu, J., Pang, Y., Zhu, Z., Wang, D., Li, C., Huang, W., Zhu, X. and Yan, D., **2013**. Therapeutic nanocarriers with hydrogen peroxide-triggered drug release for cancer treatment. *Biomacromolecules*, *14*(5), pp.1627–1636.

187. Zhang, W., Hu, X., Shen, Q. and Xing, D., **2019**. Mitochondria-specific drug release and reactive oxygen species burst induced by polyprodrug nanoreactors can enhance chemotherapy. *Nature Communications*, *10*(1), pp.1–14.

188. Uthaman, S., Pillarisetti, S., Mathew, A.P., Kim, Y., Bae, W.K., Huh, K.M. and Park, I.K., **2020**. Long circulating photoactivable nanomicelles with tumor localized activation and ROS triggered self-accelerating drug release for enhanced locoregional chemo-photodynamic therapy. *Biomaterials*, *232*, pp.1–13.

189. Wang, Q., Guan, J., Wan, J. and Li, Z., **2020**. Disulfide based prodrugs for cancer therapy. *RSC Advances*, *10*(41), pp.24397–24409.

190. Jiang, Z. and Thayumanavan, S., **2020**. Disulfide-containing macromolecules for therapeutic delivery. *Israel Journal of Chemistry*, *60*(1–2), pp.132–139.

191. Bej, R., Dey, P. and Ghosh, S., **2020**. Disulfide chemistry in responsive aggregation of amphiphilic systems. *Soft Matter*, *16*(1), pp.11–26.

192. Liu, J., Pang, Y., Huang, W., Huang, X., Meng, L., Zhu, X., Zhou, Y. and Yan, D., **2011**. Bioreducible micelles self-assembled from amphiphilic hyperbranched multiarm copolymer for glutathione-mediated intracellular drug delivery. *Biomacromolecules*, *12*(5), pp.1567–1577.

193. Wang, Y., Zhang, T., Hou, C., Zu, M., Lu, Y., Ma, X., Jia, D., Xue, P., Kang, Y. and Xu, Z., **2019**. Mitochondria-specific anticancer drug delivery based on reduction-activated polyprodrug for enhancing the therapeutic effect of breast cancer chemotherapy. *ACS Applied Materials & Interfaces*, *11*(32), pp.29330–29340.

194. Yu, F., Zhang, F., Tang, L., Ma, J., Ling, D., Chen, X. and Sun, X., **2018**. Redox-responsive dual chemophotothermal therapeutic nanomedicine for imaging-guided combinational therapy. *Journal of Materials Chemistry B*, *6*(33), pp.5362–5367.

195. Bai, T., Du, J., Chen, J., Duan, X., Zhuang, Q., Chen, H. and Kong, J., **2017**. Reduction-responsive dithiomaleimide-based polymeric micelles for controlled anti-cancer drug delivery and bioimaging. *Polymer Chemistry*, *8*(46), pp.7160–7168.

196. Wang, H., Xu, M., Xiong, M. and Cheng, J., **2015**. Reduction-responsive dithiomaleimide-based nanomedicine with high drug loading and FRET-indicated drug release. *Chemical Communications*, *51*(23), pp.4807–4810.

197. Huang, C.C., Chia, W.T., Chung, M.F., Lin, K.J., Hsiao, C.W., Jin, C., Lim, W.H., Chen, C.C. and Sung, H.W., **2016**. An implantable depot that can generate oxygen in situ for cvercoming hypoxia-induced resistance to anticancer drugs in chemotherapy. *Journal of the American Chemical Society*, *138*(16), pp.5222–5225.

198. Li, Y., Lu, A., Long, M., Cui, L., Chen, Z. and Zhu, L., **2019**. Nitroimidazole derivative incorporated liposomes for hypoxia-triggered drug delivery and enhanced therapeutic efficacy in patient-derived tumor xenografts. *Acta Biomaterialia*, *83*, pp.334–348.

199. Roy, S., Kumaravel, S., Sharma, A., Duran, C.L., Bayless, K.J. and Chakraborty, S., **2020**. Hypoxic tumor microenvironment: Implications for cancer therapy. *Experimental Biology and Medicine*, *245*(13), pp.1073–1086.

200. Chen, Z., Wang, Z. and Gu, Z., **2019**. Bioinspired and biomimetic nanomedicines. *Accounts of Chemical Research*, *52*(5), pp.1255–1264.

201. Samson, A.A.S., Hong, S., Purushothaman, B., Lee, J. and Song, J.M., **2020**. Transparent tumor microenvironment: Are liposomal nanoparticles sufficient for drug delivery to hypoxic regions and clonogenic cells? *Applied Materials Today*, *19*, pp.1–12.

202. Sharma, A., Arambula, J.F., Koo, S., Kumar, R., Singh, H., Sessler, J.L. and Kim, J.S., **2019**. Hypoxia-targeted drug delivery. *Chemical Society Reviews*, *48*(3), pp.771–813.

203. Sahu, A., Kwon, I. and Tae, G., **2020**. Improving cancer therapy through the nanomaterials-assisted alleviation of hypoxia. *Biomaterials*, *228*, pp.1–29.

204. Li, Y., Jeon, J. and Park, J.H., **2020**. Hypoxia-responsive nanoparticles for tumor-targeted drug delivery. *Cancer Letters*, *490*, pp.31–43.

205. Zhang, T.X., Zhang, Z.Z., Yue, Y.X., Hu, X.Y., Huang, F., Shi, L., Liu, Y. and Guo, D.S., **2020**. A general hypoxia-responsive molecular container for tumor-targeted therapy. *Advanced Materials*, *32*(28), pp.1–11.

206. Yu, J., Zhang, Y., Ye, Y., DiSanto, R., Sun, W., Ranson, D., Ligler, F.S., Buse, J.B. and Gu, Z., **2015**. Microneedle-array patches loaded with hypoxia-sensitive vesicles provide fast glucose-responsive insulin delivery. *Proceedings of the National Academy of Sciences of the United States of America*, *112*(27), pp.8260–8265.

207. He, H., Zhu, R., Sun, W., Cai, K., Chen, Y. and Yin, L., **2018**. Selective cancer treatment via photodynamic sensitization of hypoxia-responsive drug delivery. *Nanoscale*, *10*(6), pp.2856–2865.

208. Confeld, M.I., Mamnoon, B., Feng, L., Jensen-Smith, H., Ray, P., Froberg, J., Kim, J., Hollingsworth, M.A., Quadir, M., Choi, Y. and Mallik, S., **2020**. Targeting the tumor core: Hypoxia-responsive nanoparticles for the delivery of chemotherapy to pancreatic tumors. *Molecular Pharmaceutics*, *17*(8), pp.2849–2863.

209. Yan, Q., Guo, X., Huang, X., Meng, X., Liu, F., Dai, P., Wang, Z. and Zhao, Y., **2019**. Gated mesoporous silica nanocarriers for hypoxia-responsive cargo release. *ACS Applied Materials & Interfaces*, *11*(27), pp.24377–24385.

210. Deng, Y., Yuan, H. and Yuan, W., **2019**. Hypoxia-responsive micelles self-assembled from amphiphilic block copolymers for the controlled release of anticancer drugs. *Journal of Materials Chemistry B*, *7*(2), pp.286–295.

211. Deng, J., Liu, F., Wang, L., An, Y., Gao, M., Wang, Z. and Zhao, Y., **2019**. Hypoxia- and singlet oxygen-responsive chemo-photodynamic micelles featured with glutathione depletion and aldehyde production. *Biomaterials Science*, *7*(1), pp.429–441.

212. Huang, J., Wu, Y., Zeng, F. and Wu, S., **2019**. An activatable near-infrared chromophore for multispectral optoacoustic imaging of tumor hypoxia and for tumor inhibition. *Theranostics*, *9*(24), pp.7313–7324.

213. Im, S., Lee, J., Park, D., Park, A., Kim, Y.M. and Kim, W.J., **2019**. Hypoxia-triggered transforming immunomodulator for cancer immunotherapy via photodynamically enhanced antigen presentation of dendritic cell. *ACS Nano*, *13*(1), pp.476–488.

214. Zhang, X., Wu, M., Li, J., Lan, S., Zeng, Y., Liu, X. and Liu, J., **2018**. Light-enhanced hypoxia-response of conjugated polymer

nanocarrier for successive synergistic photodynamic and chemotherapy. *ACS Applied Materials & Interfaces*, *10*(26), pp.21909–21919.

215. Cui, D., Huang, J., Zhen, X., Li, J., Jiang, Y. and Pu, K., **2019**. A semiconducting polymer nano-prodrug for hypoxia-activated photodynamic cancer therapy. *Angewandte Chemie-International Edition*, *58*(18), pp.5920–5924.

216. Zhang, K., Zhang, Y., Meng, X., Lu, H., Chang, H., Dong, H. and Zhang, X., **2018**. Light-triggered theranostic liposomes for tumor diagnosis and combined photodynamic and hypoxia-activated prodrug therapy. *Biomaterials*, *185*, pp.301–309.

217. Chen, D., Tang, Y., Zhu, J., Zhang, J., Song, X., Wang, W., Shao, J., Huang, W., Chen, P. and Dong, X., **2019**. Photothermal-pH-hypoxia responsive multifunctional nanoplatform for cancer photo-chemo therapy with negligible skin phototoxicity. *Biomaterials*, *221*, pp.1–11.